REMOVAL OF METHYL ORANGE DYE BY *LEMNA MINOR* (DUCKWEED) AND THE EVALUATION OF ECOTOXICITY OF THE DYE USING EARTHWORM

(PROJECT REPORT)

Submitted in partial fulfillment of the requirements for the award of Bachelor of Technology Degree in **Biotechnology**

By

SWATHY T (38230038)

DEPARTMENT OF BIOTECHNOLOGY

SCHOOL OF BIO & CHEMICAL ENGINEERING

SATHYABAMA

INSTITUTE OF SCIENCE AND TECHNOLOGY

(DEEMED TO BE UNIVERSITY)

Accredited with grade "A" by NAAC

JEPPIAAR NAGAR, RAJIV GANDHI SALAI, CHENNAI – 600119

MAY - 2022

SATHYABAMA
INSTITUTE OF SCIENCE AND TECHNOLOGY
(DEEMED TO BE UNIVERSITY)
Accredited "A" Grade by NAAC | 12B Status by UGC | Approved by AICTE
www.sathyabama.ac.in

DEPARTMENT OF BIOTECHNOLOGY

BONAFIDE CERTIFICATE

This is to certify that this Project Report is the bonafide work of **Swathy T (38230038)** who carried out project entitled **Removal of Methyl Orange Dye by *Lemna minor* (Duckweed) and the Evaluation of Ecotoxicity of the Dye using Earthworm** under my supervision from **January 2022** to **April 2022**.

Internal Guide	**External Guide**
DR. M. BAVANILATHA	DR. P. PRAKASH

Head of the Department

DR. V. RAMESH KUMAR

Submitted for Viva voce Examination held on_____

Internal Examiner **External Examiner**

DECLARATION

I **Swathy T** hereby declare that the Project entitled **Removal of Methyl Orange Dye by *Lemna minor* (Duckweed) and the Evaluation of Ecotoxicity of the Dye using Earthworm** done by me under the guidance of **Dr. M. Bavanilatha (Internal Guide)** and **Dr. P. Prakash (External Guide)** at **Sathyabama Institute of Science & Technology** is submitted in partial fulfillment of the requirements for the award of **Bachelor of Technology** degree in **Biotechnology.**

DATE: 21.04.2022

PLACE: Chennai **SIGNATURE OF THE CANDIDATE**

ACKNOWLEDGEMENT

I am pleased to acknowledge my sincere thanks to Board of Management of SATHYABAMA for their kind encouragement in doing this project and for completing it successfully. I am grateful to them.

I convey my thanks to **Dr. V Ramesh Kumar, Head of the Department, Dept. of Biotechnology** for providing me necessary support and details at the right time during the progressive reviews.

I would like to express my sincere and deep sense of gratitude to my Project Guide **Dr. M. Bavanilatha (Internal Guide)** and **Dr. P. Prakash (External Guide)** for their valuable guidance, suggestions and constant encouragement paved way for the successful completion of my project work.

I wish to express my thanks to all Teaching and Non-teaching staff members of the Department of **Biotechnology** who were helpful in many ways for the completion of the project.

ABSTRACT

A textile industry's use of dyes and pigments for coloring can lead to the deposition of many toxic substances in aquatic environments. Thus, ecologists are particularly interested in developing novel sorbents capable of removing organic pollutants from wastewater. The present study deals with the utilization of this widely available aquatic *Lemna minor* (duckweed) dry biomass as sorbent in the removal of methyl orange dye from an aqueous solution and to check the ecotoxicity of the dye on earthworms. Methyl orange dye is one of the synthetic diazo groups, which is widely used in the textile, food and paper industries. SEM, GC-MS analysis and FTIR studies were evaluated at various stages to confirm the sorption of methyl orange over the aquatic sorbent material. The dye concentration was evaluated using a spectrophotometer with a wavelength of 464nm. The kinetics, isotherm studies were performed to study the interactive mechanism of duckweed adsorbent with methyl orange dye. Isotherm models like Langmuir, Freundlich, Langmuir-Freundlich and Temkin models are evaluated to determine the equilibrium dye adsorption concentration. This enhances the sorption capacity of the methyl orange dye molecule as supportive with other literature. Maximum adsorption concentration was found out. In order to determine how the dye was toxic for the environment, ecotoxicity tests were conducted.

TABLE OF CONTENTS

LIST OF ABBREVIATIONS

SEM – Scanning Electron Microscope

GCMS – Gas Chromatography and Mass Spectrometry

FTIR – Fourier Transformation InfraRed Spectroscopy

MB – Methylene Blue

AR88 – Acid Red 88

AO74 – Acid Orange 74

HPL – HCl-pretreated *Lemna sp.*

AgNP – Silver Nanoparticles

rpm – Rotation Per Minute

NBS – National Bureau of Standards

min. – minutes

pH – negative logarithm of hydrogen

UV-Vis – Ultraviolet Visible Spectrophotometer

BR46 – Basic Red 46

AB113 – Acid Blue 113

NaOH – Sodium Hydroxide

HCl – Hydrochloric Acid

$K_2Cr_2O_7$ – Potassium Dichromate

AF-MnP – Amino Functionalized Magnetic Nanoparticles

SG3 – Solvent Green 3

ABTS – [2,2'-azino-bis(3-ethylbenzothiazoline-6-sulfonic acid)]

COD – Chemical Oxygen Demand

TDS – Total Dissolved Solids

TN – Total Nitrogen

EC – Electrical Conductivity

TP – Total Phosphorous

CR – Congo Red

CV – Crystal Violet

RH-B – Rhodamine-B

ANOVA – Analysis of Variance

EDX – Energy Dispersive X-ray analysis

FE-SEM – Field Emission Scanning Electron Microscopy

Co_3O_4 – Cobalt Oxide

XRD – X-ray Powder Diffraction

MO – Methyl Orange

TRAC – Tobacco Residue Activated Carbon

CCD – Central Composite Design

RSM – Response Surface Methodology

Conc. – Concentration

Abs. – Absorbance

LIST OF TABLES

LIST OF FIGURES

1 INTRODUCTION

In a rapidly developing economy, industries release pollutants that pose a threat to the environment. Water pollution is one of the most serious threats to the environment. The textile, pulp and paper, plastics, drug, and traditional batik industries produce large amounts of dyes containing wastewater (Imron et.al. 2021). Dyes are are organic compounds that are capable of coloring other substances (Balarak et.al. 2015). Despite their useful properties, dyes exert negative impacts on water systems as a result of their structure or origin, which differ according to chemical forms. These chemical forms include acidic, reactive, basic, dispersed, azo, diazo, anthraquinone-based, and metal-complex dyes, among others. Metal-complex azo acid dyes are used widely in textiles due to their light and wetfast properties. Azo dyes are the most important group of synthetic dyes (Reyes-Ledezma et.al. 2020).

The dyes must be removed from wastewater as soon as possible to prevent the release of these dyes into the environment. Benzidine and naphthalene are the main carcinogens in these dyes, so it is vital to treat these high volumes of wastewater. When these dyes enter biological systems, such as animals and humans, they can be absorbed as mutagens and carcinogens following microbial degradation (Marimuthu et.al. 2020; Khandare 2015). There are many physical, chemical, and biological methods for the treatment of dye-containing wastewater. These include adsorption, biosorption, coagulation, precipitation, membrane filtration, solvent extraction and chemical oxidation (Chakravarty et.al. 2008). For the removal of dyes from wastewater, the adsorption technique has been found to be the most prominent method (Dogan et. al. 2008). A number of alternative adsorbents are developed and used to remove colour from aqueous solutions due to the high cost of activated carbon (Diyanati and Balarak 2013). Methyl orange is an organic dye mainly used in textile industry.

Fig. 1.1: Methyl Orange Dye

Since a few years, phytoremediation has been employed as a unique strategy in dye degradation; it involves the employment of plants and rhizospheric microbes to remove hazardous substances from contaminated locations. Many plants have been examined for their phytoremediation potential in textile wastewater treatment, however most of them are still in the lab (Chandanshive et.al. 2020). It implies growing plants for a specified amount of time in a contaminated matrix in order to remove contaminants from the matrix. By functioning as filters, plants can absorb organic contaminants (Bianchi et.al. 2011).

The common duckweed (*L. minor*) is a harmful floating aquatic macrophyte that has ecological and economic consequences wherever it grows (Ekperusi et.al. 2019). *Lemna minor* is a little free-floating macrophyte that develops quickly and fits well to a variety of aquatic situations, such as stagnant ponds or slow-moving streams. Pollutants from wastewater can be accumulated and absorbed by this plant. Heavy metals are also removed from industrial and textile wastewaters using this method. Furthermore, it is a useful source of fodder due to its high protein content and less fibre content (Yaseen et.al. 2016). They thrive as a result of the disposal of artificial fertilizers in farm lands and drainage water, which damages the environment with nitrogen and phosphorus

compounds, contributing to the growth of water plants on the water's surface as a result of eutrophication (Prakash et.al. 2021). *L. minor* is useful for phytoremediation because it adapts more to a variety of aquatic conditions, grows quickly, and can absorb pollutants (Can-Terzi et.al. 2021).

Fig. 1.2: Lemna minor

The current work looks at using aquatic duckweed as an adsorbent to remove the methyl orange dye from aqueous solution, which is a common water-soluble anionic dye. The sorption of methyl orange dye over the aquatic sorbent material was confirmed by SEM, GC-MS analysis, and FTIR tests at various stages. The interaction mechanism of duckweed adsorbent with methyl orange dye was investigated using kinetics and isotherm analyses. To calculate the equilibrium dye adsorption concentration, isotherm models such as Langmuir, Freundlich, Langmuir-Freundlich, and Temkin are evaluated. As evidenced by other publications, this improves the sorption capability of the methyl orange dye.

2 REVIEW OF LITERATURE

The effects of plant weight, contact time, and initial Methylene Blue concentration were investigated in a batch reactor experiment with three replicates. The number of reactors utilised was 70, with a weight of 2g, an efficiency of 82.48 ± 1.09% (2 days), and an initial concentration of 50mg/L. The adsorption of MB on numerous plant weight is explained by pseudo-second order kinetics, and the MB absorption capacity is explained by the Freundlich isotherm. The FTIR results are important in phytosorption of MB and biodegradation of MB, resulting in phenol and amine (Imron et.al. 2021).

An experimental study was conducted to evaluate the potential of Lemna minor in the removal of Acid Red 88 dye. The effect on Acid Red 88 dye removal was investigated by selecting the most effective variable, it included contact time (15-180min), pH (3-11), adsorbent dose (0.1-1g/100mL), and initial dye concentration (25-500mg/l). The effect of contact time and initial AR88 concentration, as well as the effect of adsorbent dose and pH, were studied, and it was found that the dye removal density (mg/g) increased with time (Balarak, Pirdadeh & Mahdavi 2015).

The molecular structure and primary properties of Acid Orange 74 (AO74) is evaluated in order to evaluate HCl-pretreated Lemna sp. (HPL) as a biosorbent of AO74 in water. The zeta potential of HPL suspensions was measured at room temperature (rt) and at various pH levels (1–11). Biosorption, desorption, FTIR, SEM, and pseudo-second-order model kinetics were used to conclude that AO74 dye was entirely removed by HPL and not by abiotic factors (Reyes-Ledezma et.al. 2020).

Mechanisms of dye removal using AgNPs were evaluated, including dye adsorption on AgNP-loaded activated carbon, photocatalytic degradation, and a mixture of the two. As per study, AgNP-loaded activated carbon had the highest adsorption of 71.4mg of methylene blue adsorbent. Acetone desorption resulted in 86% reusability of the novel adsorbent. The MB adsorption kinetics followed the pseudo-second-order model, and the Langmuir isotherm was suitable for the adsorption process, summarising the importance of green synthesis of AgNPs and their applications in dye effluent treatment (Marimuthu

et.al. 2020).

Color removal was investigated utilising dyes' distinctive light absorption, where each characteristic chromophores in textiles imparts colours to compounds. Each dye has its own absorbance maxima (λ_{max}) at certain wavelengths of light, making it easy to track dye elimination over time. Adsorption and UV photolysis are proposed for the treatment of textile dye effluents, with various degrees of colour removal from dye wastewaters, however there are severe worries regarding the toxicity of treated effluents, making them plainly inadvisable. Microorganisms are used because of their dynamic metabolisms and ability to adapt to harmful pollutants in the environment. The efficiency of microbial decolorization is largely dependent on the compliance and activity of prospective bacteria, implying that plants from a diverse range of environments have been demonstrated to be exceptionally promising bioremediation techniques for textile dyes and associated effluent (Khandare and Govindwar 2015).

Adsorption experiments were conducted in batches of 50mL of Cu(II) solution with specified weights of newspaper pulp, and the influence of pH on adsorption was studied by changing the pH range from 2–7 using dilute NaOH and HCl. Kinetic and thermodynamic studies were performed for three different Cu(II) concentrations at temperatures of 30, 40 and 50°C and instrumentation was performed using an atomic absorption spectrophotometer, demonstrating that newspaper pulp is a potential adsorbent for Cu based on the pH, pseudo second order kinetic model for the entire temperature range. E_a (activation energy) reveals that Cu adsorption is an endothermic and spontaneous process (Chakravarty et.al. 2008).

Adsorption studies were carried out in batches using Methylene Blue solution made with ultrapure water. 50mL of dye solution in 100mL conical flasks was agitated in a rotary shaker for 24 hours at 200rpm with 0.25g of hazelnut shell at specified pH and temperature. Before each measurement, the pH was adjusted with 0.1N HCl and 0.1N NaOH using a pH meter and calibrated using NBS buffers. The effects of pH and temperature were studied before centrifuging the solution for 10 minutes at 5000rpm. Following centrifugation, the dye concentration in the supernatant solution was determined using a UV-vis spectrophotometer with a maximum absorbance at 663nm, indicating that

hazelnut shell has enough adsorption capacity for the removal of MB from its aqueous solution (Dogan et.al. 2008).

Batch adsorption was performed using an initial acid orange 7 concentration and the effects of absorbent dose, contact duration, and pH were investigated. The batch system studies were carried out in a 100ml Erlenmeyer flask. A specific concentration of AO7 and a specific dosage of absorbent are put into the flask and thoroughly mixed with a shaker at 120rpm for 180min, followed by centrifugation at 3600rpm for 10 minutes. Finally, residual concentrations were determined using a Spectrophotometer at a maximum of 452nm, indicating that dried Rice Stem may be employed as an effective adsorbent to treat dye-containing effluent dependent on starting dye concentration, adsorbent dosage, pH, and contact duration **(**Diyanati and Balarak 2013).

Plant material and chemicals were selected, textile dye was decolorized by *V.zizanioides*, photosynthetic pigments and plant histology were investigated, enzyme extracts were prepared, phytodegraded products were extracted and evaluated, the toxicity of Remazol Red and its products was assessed, a floating phyto-bed reactor of *V.zizanioides* was built, textile wastewater treatment in planted furrows was assessed, and it was concluded that the combinatorial plantation of *V.zizanioides* (Chandanshive et.al. 2020).

Phytoremediation in air, soil, and water was investigated, and the use of macrophytes in water was discovered. The role of constructed wetlands in macrophytes and phytoremediation in macrophytes were investigated, and it was calculated that among the macrophytes, the common duckweed, L.minor, has been widely used in agriculture, pharmaceuticals, biofuels, toxicity testing, environmental monitoring, and bioremediation of a wide range of chemical pollutants in wastewater effluents and aquatic ecosystems (Ekperusi, Sikoki and Nwachukwu 2019).

Simple plastic washing-up containers were used to degrade the dye. Each Basic Red 46 dye was assigned 11 containers (6 with dye + 5 without dyes) and monitored. Each container was filled to the required level with tap water. Following that, 200 healthy L.minor plants were placed to each container, and the system was watered and fertilised regularly. Spectrophotometer analysis of standard water quality for COD, absorbance, apparent colour, and suspended particles revealed that the shallow ponds eliminated the BR46

under semi-natural settings (Yaseen and Scholz 2016).

Lemna minor was collected from the pond and rinsed thrice with tap water before being powdered and sieved at 75m after being shade dried for three days. By adjusting the concentration and controlling the pH using NaOH (0.1N) and HCl, the impact of acid blue dye 113 concentration was examined (0.1N). 1g of *Lemna minor* powder was weighed into 250mL conical flasks before 100mL of AB113 solution was added to each flask. The adsorbent was shaken continuously (0–60min) and the solution centrifuged to establish the equilibrium, which was then assessed using UV-Vis. pH, contact time interval, dye concentration, temperature, biosorbent amount and Kinetic investigations enhance the biosorbent's parametric assessment at 98.5% removal capacity, resulting in the conclusion that the biosorbent successfully eliminates AB113 (Prakash et.al. 2021).

By collecting leaves, sun-drying and sieving the powder, and dissolving K2Cr2O7 in deionized water, the integration of C.dactylon (L1) and M.koenigii (L2) plant extracts was examined. The morphological features of amino-functionalised magnetic NP integrated with L1 and L2 were studied using TEM and SEM to investigate its size, elemental contents, and magnetic properties. Magnetic NPs were created by dissolving 100 ml of deionised water in a 1:1 mixture of FeCl3.6H2O and FeSO4.7H2O. The polyphenols were extracted using a Soxhlet extractor after AF-MnP-L1 and L2 were mixed with 250ml of ethanol. Optimisation, Adsorption isotherm, and Kinetics were carried out, indicating that green adsorbent efficiently treats industrial effluents (Vishnu and Dhandapani 2020).

Studying the structure and properties of Solvent Green 3 allows Anthraquione Dye Green 3 to be detoxified. *Hortaea sp.* was cultured in the Bushnell–Haas (BH) liquid medium augmented with SG3 to study microbes and culture conditions. The UV–vis characterisation by change in peaks between treated dye samples and controls was used for the decolorization study. Laccase activity was determined by measuring the absorbance at 420nm of a reaction mixture containing ABTS in sodium acetate buffer ($\text{Ɛ}420 = 36{,}000 M^{-1} cm^{-1}$). TLC was used to evaluate SG3 metabolites, which were then sprayed with p-anisaldehyde to detect acidic chemicals, resulting in the conclusion that *Hortaea sp.* totally destroyed SG3 (Al Farraj et.al. 2019).

Microalgae were used to cultivate sodium alginate composites, and nutrient absorption

capability was determined by inoculating a pure culture of Chlorella strain in wastewater and measuring COD, TDS, TN, EC, pH, and TP. The dried *Chlorella* biomass was ground, sieved, and submerged in 5% HCl and NaOH at 120rpm for 12h before filtering the treated matter for 12h. The Na-Alg/Ch conjugate was made by dissolving 2g Na-Alg in 100mL water and heating and chilling the combination. The HCl-treated *Chlorella* mass was then poured into 0.1M $CaCl_2$ solution, resulting in dropwise beads. According to the results of the adsorption capacity, temperature, contact time, beginning dye concentration, pH, and desorption studies, the conjugate is used for the adsorptive removal of CR dye (Maqbool et.al. 2021).

Cucumis sativus removes dyes from aqueous systems by crushing the fruit peel, drying in an oven, treating with concentrated H_2SO_4 for 12h, rinsing thoroughly with distilled water until it reaches neutral pH, then soaking in 2% $NaHCO_3$ overnight to remove any surplus acid. The surface charge of chemically and microwave activated adsorbents at varied solution pH levels was investigated using zero-point charge determination. The influence of pH, contact duration, adsorbent dosage, adsorption kinetics, and adsorption isotherm of Crystal Violet and Rhodamine-B was evaluated in a batch method, with the conclusion that *C.sativus* adsorbent removes CV and RH-B from aqueous solutions (Smitha et.al. 2017).

Sorbent Dosage was studied using an equal distribution of 1800mL of dye solution (10mg/L concentration) in five 300mL conical flasks. The accumulation tests were carried out by adjusting the sorbent dose from 1–3g wet weight, withdrawing samples on a daily basis, centrifuging at 12000rpm for 10 minutes once equilibrium was attained, and measuring the supernatant absorbance using a UV-spectrophotometer. The effect of pH on plant development and MB dye absorption capability was investigated by altering the pH range from 3–8 and examining the initial dye concentration for 6 days until equilibrium was attained along with dye accumulation. Duckweed was shown to be a promising plant for the bioaccumulation of basic dye from aqueous solution based on statistical analysis using one way ANOVA (Reema et.al. 2011).

Co_3O_4-NP were created by dissolving 1g of Pluronic F-127 in 100mL of water, then stirring continuously for 30 minutes with a magnetic stirrer, adding $CoNO_3$ solution, and finally

adding 2M NaOH (100mL). FE-SEM pictures of the synthesised $Co3O_4$-NP before and after methyl orange dye adsorption were captured using a TESCAN FE-SEM operating at 20kV, followed by EDX and mapping given by EDX equipment connected to the FE-SEM apparatus. FTIR spectra, TEM images, and XRD patterns were all captured. Adsorption tests were performed by dissolving 0.5g $Co3O_4$-NP in 50mL of MO solution containing C_i and a certain pH value. C_f was measured using a UV spectrophotometer set at 460nm. RSM was examined, and it was determined that Co_3O_4-NP degrades MO the best (Uddin and Baig 2018).

Activated carbon is used to absorb binary dyes from tobacco residues. This experiment was done out by producing Tobacco Residue Activated Carbon and analysing it using SEM, FTIR and XRD. The stock solutions were made by dissolving different quantities of each dye (0.0025, 0.005, 0.0075, 0.01 and 0.0125g) in a 50mL water flask to get (50, 100, 150, 200 and 250ppm) solutions, then combining each dye in different ratios (1:1, 1:1.6 and 1:2) in 50mL water. Central Composite Design (CCD) was used to study ultrasound-assisted batch adsorption. TRAC adsorbed MB and AB25 dyes were shown to have TRAC adsorbed MB and AB25 dyes based on equilibrium modelling, kinetics, and thermodynamic **analyses (Archin, Sharifi, Asadpour 2019).**

The ability of duckweeds (*L. minuta* and *L. minor*) to remove nutrients from simulated wastewater was investigated using an experimental design that included sample collection, morphological analysis, and enrichment with 3g of KNO_3 and 4g of KH_2PO_4. The physicochemical analysis was examined by utilising an immersion multi-probe to measure water temperature, pH, conductivity, and dissolved oxygen. During the experiment, variations in *Lemna* thickness (mm) and weight (g) were evaluated to assess biomass production. Nitrate and phosphate levels, as well as chlorophyll and malondialdehyde content, were determined in *Lemna* fronds, suggesting that *L. minuta* is more effective than *L. minor* in nutrient removal (Ceschin, Crescenzi and Iannelli 2020).

Lemna minor degrades Toluidine Blue (TB) from aqueous solution in batch studies at room temperature (252°C) by diluting the plants with TB solutions at different initial concentrations ranging from 5–40mg/L. The concentration of TB in solution was determined using a T70 UV-Vis spectrophotometer (λ_{max} = 633 nm) by measuring the

absorbance of solutions with known concentrations (2, 4, 6, 8, 10mg/L) which concludes that *Lemna minor* has a high capacity for adaptation in a polluted environment and can be used for industrial wastewater treatment (Neag, Malschi & Măicăneanu 2018).

RSM is used to improve the integrated chemical–biological degradation of a reactive azo dye. This experiment was conducted using a reactor setup in which the initial H_2O_2 dose, UV irradiation period, and recirculation from the bioreactor to the photoreactor determined the best conditions for degrading Acid Red195 dye. Analytical methods were used to avoid incorrect results by removing Residual H_2O_2 before soluble COD, followed by optimization of the integrated chemical–biological treatment to degrade RR195 using RSM design, which summarises the usefulness and effectiveness of the RSM in predicting system performance and maximising dye degradation by using integrated chemical and biological treatment process (Sudarjanto et.al. 2006).

To convert duckweed biomass to ethanol, duckweed species are selected and cultured in a laboratory at a constant temperature (23°C) and under 12h lighting (white fluorescent light), followed by enzymatic saccharification in two-step hydrolysis (50mg of dry powder + 1mL of 25mM CH_3COONa + 480µL α-amylase + 20µL α-amyloglucosidase) and one-step hydrolysis (50mg of dry powder + 1mL of 25mM CH_3COONa). Ethanol fermentations were carried out in micro-bioreactors using the self-flocculating yeast strain SPSC01 (Ge et al. 2005) and an ATCC 24859 *S. cerevisiae* strain (Ge et.al. 2012). The biomass and culture medium composition assays were performed, resulting in the conclusion that *L. minor* has a high potential for converting pollutants into a biofuel production system (Ge et.al. 2012).

Lemna minor removes chromium ions from wastewater. This method is carried out by choosing the plant material, washing it multiple times with tap water to remove dirt, sludge, and other debris, and then placing it in a pilot system consisting of three 14L plexiglas ponds filled with Synthetic Duckweed Nutrient Solution. The pilot system is carried out in three ponds (two with DNS and Cr^{2+} ions and one without metal) and is followed by an evaluation of plant growth rates, dry/fresh weight ratios, and chlorophyll contents, which concludes that the capacity of aquatic plants to remove potentially toxic heavy metals, including chromium, from water is well documented (Uysal 2013).

3 AIM AND SCOPE OF THE PRESENT INVESTIGATION

3.1 AIM:

- To investigate the removal of methyl orange dye using the *Lemna minor* (Duckweed)
- To check the ecotoxicity of the dye

3.2 OBJECTIVE:

- To prepare the bio-adsorbent
- To characterize the adsorbent interaction using FTIR, GC-MS, Kinetic and isotherm studies
- To determine the equilibrium dye adsorption concentration using Isotherm models like Langmuir, Freundlich, Langmuir-Freundlich and Temkin models
- To find out the maximum adsorption
- To find out the ecotoxicity of the dye adsorbed *Lemna minor* (Duckweed) adsorbent

4 METHODOLOGY

4.1 SAMPLE COLLECTION

The duckweeds (*Lemna minor*) were collected from the eutrophicated pond in Thirumalai Nagar, Hasthinapuram and washed thrice with tap water.

Fig:4.1: Collection of Lemna minor and shade dry

4.2 ADSORBENT PREPARATION

To remove the moisture content, shade drying processing was done for 3 days. The dried duckweeds were powdered by using a mixer grinder and finally sieved to particle size in the range of 150µm. The stock of 500mg/L of Methyl Orange dye was prepared initially and diluted in 1000mL distilled water. The experimental solution was obtained by dilution of the working solution at desired concentrations (100ppm–2000ppm).

Fig: 4.2 Ground Lemna minor powder

4.2 ADSORBATE

The adsorbate utilized is methyl orange dye that is most ordinarily utilized in textile industry and released in wastewater

1. *Methyl orange:*
    1. *Molecular formula:* $C_{14}H_{14}N_3NaO_3S$
    2. *Molecular weight: 327.34g/mol*
    3. *IUPAC name:* sodium;4-[[4-(dimethylamino)phenyl]diazenyl]benzenesulfonate

4.3 PROPERTY ANALYSIS OF THE ADSORBENT

4.3.1. ***Moisture content determination****:* 1g of the adsorbent was collected and dried in an oven for 4 hours at 150°C. The moisture content was calculated from the following formula:

$$X_o = \frac{W_1 - W_2}{W_1}$$

X_o = Moisture content on wet basis

W_1 = Initial weight of sample

W_2 = Final weight of sample after drying

4.3.2 ***pH determination:*** 1g of the adsorbent was weighed and dissolved in 100ml of de-ionized water. The mixture was heated and stirred for 3minutes to ensure proper dilution of the sample. The solution was filtered and its pH was determined using a digital pH meter.

4.3.3 ***Determination of Porosity and Bulk Density:*** The adsorbent (1g) was dispersed in 20ml water in a graduated cylinder with the aid of a shaker, this was further centrifuged for 10min. The resulting volume of the water was read and recorded. The equation below was used for the calculation of the porosity and bulk density:

$$\text{Porosity} = \frac{V_w}{V_T}$$

$$\text{Density} = \frac{R_{aw}}{1 - \alpha}$$

$$R_{aw} = \frac{M_a}{V_w}$$

V_w – Volume of supernatant

V_T – Total volume of adsorbent

M_a – Mass of adsorben

4.3.4 ***Pore Volume:*** The adsorbent (1g) was transferred into a 10ml measuring cylinder in order to get the total volume of the sample. The sample was then poured into a beaker containing 20ml of deionized water and boiled for 5min. The content in the beaker was then filtered, superficially dried, and weighed. The pore volume of the sample was determined by dividing the increase in weight of the sample by the density of water.

4.3.5 ***Phytochemical analysis:*** 1g of duckweed was combined with 100ml of deionized water before being filtered and analyzed for phytochemicals.

4.3.5.1 *Phlobatannins:* 1mL of *Lemna minor* adsorbent was placed in a boiling tube and heated with 2mL of 1% aqueous hydrochloric acid. To produce color, this combination was let to stand for a few seconds or minutes. The existence of Phlobatannins is confirmed by the appearance of red precipitate.

4.3.5.2 *Saponin:* 2mL of *Lemna minor* adsorbent solution was placed in a boiling tube and boiled with 20mL of distilled water before being filtered. 10ml of filtrate was added to 5ml of distilled water and aggressively shaken for the appearance of stable persistent foam. Three drops of olive oil were added to the foaming mixture and rapidly agitated to form the emulsion. It is accepted as proof of the existence of Saponin.

4.3.5.3 *Flavonoids:* 5ml of dilute ammonia solution was added to the aqueous filtrate of the *Lemna minor* adsorbent, and then modified or developed the color by adding strong sulphuric acid to the mixture. The presence of flavonoids is confirmed by the presence of yellow color.

4.3.5.4 Steroids: To 0.5ml of *Lemna minor* adsorbent, 2ml of acetic anhydride was added, followed by addition of 2ml of sulphuric acid and the reaction takes place. The development of green or violet to blue proves the presence of steroids.

4.3.5.5 Terpenoids (Salkowski test): In a test tube, 5ml of *Lemna minor* adsorbent was taken and 2ml of chloroform was added to it, followed by careful addition 3ml of concentrated sulphuric acid through it to form a layer. Appearance of reddish-brown colour confirms the presence of terpenoids.

4.3.5.6 Glycosides (Keller-Kiliani test): 2ml of glacial acetic acid was mixed with 5ml of *Lemna minor* adsorbent, followed by addition of one drop of ferric chloride solution and 1ml of concentrated sulphuric acid in test tube. Appearance of brown ring at the interface confirms Glycosides (Antony Samrot 2009).

4.3.5.7 Tannins: In a boiling tube, 0.5mL of *Lemna minor* adsorbent was placed and boiled with 20mL of water before being filtered alongwith addition of few drops of 0.1% ferric chloride. The presence of tannins is indicated by the appearance of brownish green or a blue-black tint.

4.3.6 ***Electrical Conductivity:*** 1g of adsorbent was weighed and added in 100ml deionized water. The solution was filtered, and the pH was measured with a digital EC meter.

4.3.7 ***Protein estimation:*** In 100ml of deionized water, 1g of duckweed powder was added. The mixture was then centrifuged, filtered, and analyzed using Lowry's technique to determine the protein concentration.

4.4 INITIAL CONCENTRATION AND THE ABSORBANCE OF THE METHYL ORANGE DYE

1g of methyl orange in 1000ml equals 1000ppm. Using methyl orange dye, concentrations ranging from 100ppm to 2000ppm were achieved. At 464nm, absorbance was measured using a UV spectrophotometer with a dilution factor of 12.

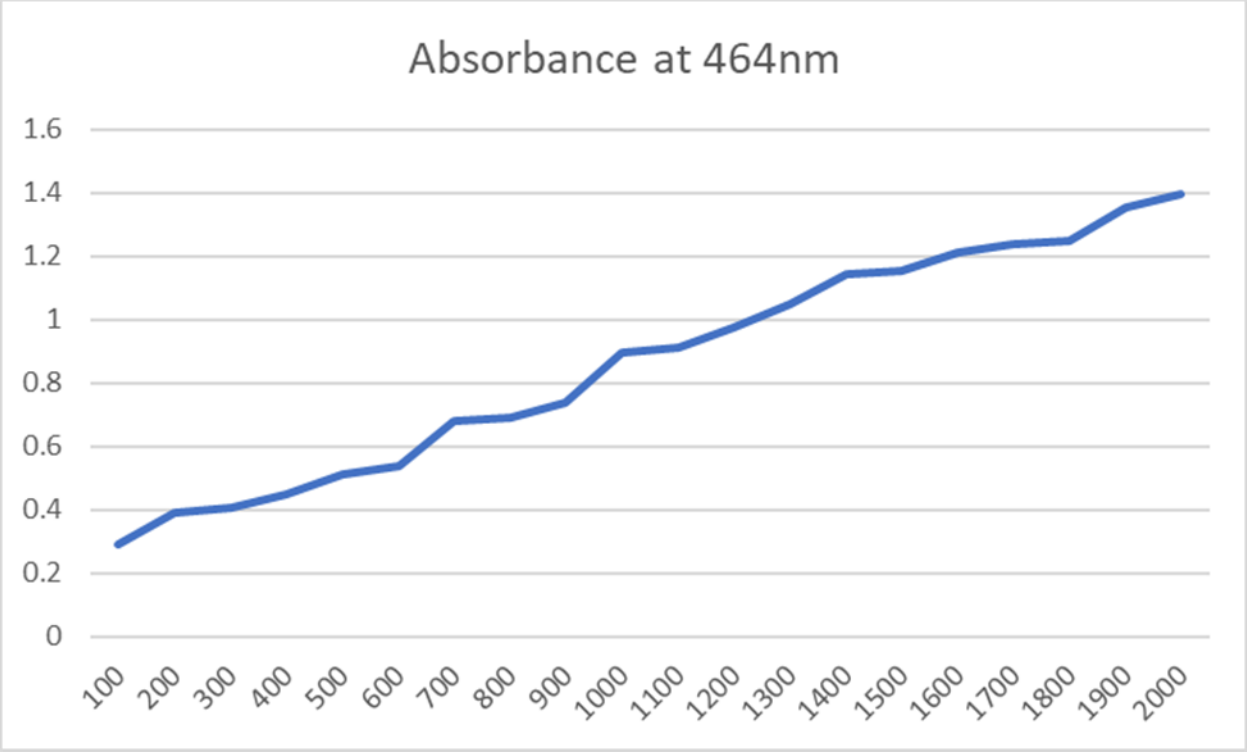

Fig. 4.3: Absorbance of dye at 464nm

4.5 **DYE DEGRADATION:** The batch approach was used to investigate the adsorption and degradation of methyl orange dye using a low-cost adsorbent, duckweed. 1g of dye was dissolved in 1000ml of water to make a stock solution of 1000mg/L. The resulting solution was diluted to different ppms. The UV visible spectrophotometer was used to get standard values for all of these solutions at 464nm. All dye solutions with varying concentrations received 1g of the substrate. A portion of each solution was promptly filtered, and UV measurements at 464

nm were obtained to calculate the adsorption percentage. The leftover solutions were placed in a shaker incubator, and the process was repeated until a consistent UV reading was obtained on two consecutive days. The formula was used to determine the absorption percent and degradation percent based on the standard and absorbance readings.

$$\%\text{Adsorption and }\%\text{Degradation} = \frac{C_o - C_f}{C_o} \times 100$$

C_o – Initial Concentration of the Dye

C_f – Final Concentration of the Dye

Initial tests were done at lower ppm. Assuming the outcomes are positive, higher ppm were utilized for the review.

4.6 **LACCASE ACTIVITY:** Laccase activity was measured using the ABTS technique for two consecutive days for various concentrations of duckweed-added methyl orange dye solution ranging from 100ppm to 2000ppm, as well as the control. ABTS concentration of 0.1% in 100mM of pH 5 sodium acetate buffer was produced, and 3ml of the substrate was poured into the cuvette, along with 250µl of the extracts, which were centrifuged and filtered for varied concentrations. At 420nm, absorbance was measured after 1 minute of incubation (Papinutti et al 2003).

Laccase Activity (µ/ml) =

$$\frac{Absorbance\ at\ 420\ nm \times Volume\ of\ reaction\ mixture\ in\ ml \times Dilution\ factor}{Molar\ extinction\ coefficient\ of\ ABTS\ at\ 420nm \times Volume\ of\ enzyme\ in\ reaction\ mixture(ml) \times Incubation\ time}$$

Molar extinction coefficient of ABTS at 420nm = $36000 M^{-1} cm^{-1}$

4.7 **DYE DECOLORIZATION OF THE ADSORBENT:** 1.5g of methyl orange was dissolved in 1000ml of distilled water to make a dye solution with a concentration

of 1500ppm. 1g of duckweed powder was added to 100ml of dye solution at a concentration of 1500ppm and left undisturbed for 4 days. This solution was filtered and sent to be analyzed.

4.8 **MICROBIAL ANALYSIS:** After 24 hours of incubation with Muller Hinton Agar, 1ml of Aqueous duckweed extract, 48th hour extract, and control were tested for microbial growth. Microbial analysis was performed to determine if adsorption was connected to the bacteria found in the adsorbent and adsorbate combination.

4.9 **OPTIMIZATION OF PARAMETERS:** In order to optimize the significant parametric evaluation of biosorbent at its maximum removal capacity, the interaction between pH and temperature was evaluated. The dye concentration was determined using a spectrophotometer with a wavelength of 464nm (Prakash et. al. 2021).

4.10 **CHARACTERIZATION STUDIES OF THE ADSORBENT AND AFTER TREATMENT:**

4.10.2 ***SEM****:* Scanning Electron Microscopy (SEM) is a type of electron microscope that creates pictures of solid surfaces by scanning them with electron beams. Electron beams impact the atoms on the sample surface, producing a variety of signals. Electron detectors detect these impulses. These signals include information about the sample's composition and surface structure. Duckweed surface morphology and adsorbed duckweed surface morphology were studied.

4.10.3 ***FTIR:*** FT-IR is used to determine the chemical structure of a material. Infrared radiation is passed through the sample in FTIR spectroscopy, some of which is absorbed inside the sample and part of which is passed and transmitted by the sample. The resultant spectrum from infrared absorbance and transmission by sample represented the molecule absorption and

transmission, resulting in a molecular identification image of the sample. At the radiation receiver, each molecule and chemical link produced a unique infrared spectrum. As a result, FTIR spectroscopy results in the identification (qualitative analysis) of various types of bonds and sample structure. The FTIR of duckweed before and after adsorption was performed in the current study.

4.10.4 ***GCMS:*** GCMS separates chemical mixtures (the GC component) and identifies the components at the molecular level (the MS component) as well as potential metabolites. The GC operates on the premise that when a mixture is heated, it separates into discrete components. The hot gasses are passed via a column containing an inert gas (such as helium). GCMS was used to examine the dye solution after treatment as well as the effluent before and after treatment.

4.10.5 ***UV - VIS Spectrophotometer****:* It makes use of light in the ultraviolet and visible ranges of the electromagnetic spectrum (190nm-1100nm). When a radiation beam passes through the solution, some of the light is absorbed and the rest is transmitted. The sample's absorbance is the negative logarithm of its transmittance. The concentration of dye before and after treatment is determined using absorbance. For adsorption and degradation, the maximum wavelength for methyl orange is 464nm.

4.11 **ISOTHERM MODEL AND ADSORPTION STUDIES:** The quantity of gas adsorbed on a material under constant pH and temperature with variable pressure is referred to as the adsorption isotherm. It is a function of the solid's surface area and pore structure; hence it can give important information about these two elements. Adsorption isotherms are a popular tool for characterizing porous materials. The existence of specific types of pores results in varied isotherm forms. The Langmuir and Freundlich models are the most often used

adsorption isotherm models.

4.11.2 ***Langmuir isotherm:*** This is applicable for monolayer coverage of the adsorption on the surface. In this model, adsorption is assumed to take place on homogenous surface.

$$\frac{C_e}{Q_e} = \frac{1}{Q_m}\left(\frac{1}{K_L} + C_e\right)$$

C_e – amount of dye adsorbed per unit mass of adsorbent

Q_e – concentration of dye solution at equilibrium

Q_m – adsorption capacity

K_L – Langmuir equilibrium constant

The feasibility of this model is tested by using a function called R_L (equilibrium parameter)

$$R_L = \frac{1}{1 + K_L C_0}$$

4.11.3 ***Freundlich isotherm:*** The adsorption is assumed to take place on a heterogenous surface. It is valid for multilayer adsorption.

$$\log (Q_e) = \log (K_f) + \frac{log\ (C_e)}{n}$$

Q_e – dye adsorbed at equilibrium

C_e – dye concentration at equilibrium

K_f and n – constants for a given adsorbate and adsorbent at a particular temperature

The effectiveness of every adsorption process is described by adsorption kinetics. The kinetics of dye solution adsorption at various concentrations

ranging from 100ppm to 5000ppm over a constant time interval were investigated which follows pseudo first order kinetics, pseudo second order kinetics, and so on. The following formulas were used to determine adsorption kinetics:

$$\text{Amount of dye removed at equilibrium } (Q_e) = (C_o – C_e) \times \frac{V}{m}$$

$$\text{Amount of dye removed with respect to time } (Q_t) = (C_o – C_t) \times \frac{V}{m}$$

Q_e – amount of dye removed at equilibrium

Q_t – amount of dye removed with respect to time

C_o – initial concentration

C_e – concentration of dye at equilibrium

C_t – concentration of dye at time *t*

V – volume of the dye

m – mass of the substrate

Pseudo first order kinetics:

$$\log (Q_e – Q_t) = \log Q_e – \frac{k_1}{2.303} t$$

Pseudo second order kinetics:

$$\frac{1}{Q_t} = \frac{1}{k_2 Q_{e_2}} + \frac{1}{Q_e}$$

4.11.4 ***Temkin isotherm:*** A two-parameter model for determining the heterogeneous adsorption system (Smitha et.al. 2012)

$$Q_e = B (\ln A_T + \ln C_e) = \frac{R_T}{b} (\ln A_T + \ln C_e)$$

$B = \frac{R_T}{b}$

A_T – Temkin isotherm equilibrium binding constant (l/g)

b – Temkin isotherm constant related to heat of sorption (J/mol)

R – universal gas constant (8.314 $Jmol^{-1}K^{-1}$)

T – temperature at 298K

The plot of Q_e vs. ln (C_e) enables the determination of the isotherm constants

4.12 **ECOTOXICITY USING EARTHWORM:** The biomass was prepared by filtering the adsorbent from the mixture in a tea filter, transferring the filtered residue to petri plates, and keeping the plates in a hot air oven for three days. The dried biomass was then measured from the petri plates. Two control trays and two biomass treated trays were taken and 2kg of red soil was poured into each tray. 2 trays were filled with 11g of dried biomass, and the remaining 2 trays were left as controls. A total of 10 earthworms of the species Eudrilus eugeniae were selected and placed in four trays, their weight and length was measured, and their death rates were calculated periodically (0th day, 7th day, and 14th day)

5 RESULTS AND DISCUSSION

Physical Properties: The properties of *Lemna minor* biomass, namely, moisture content, pH, pore volume and porosity were evaluated in Table 5.1.

5.1 MICROSCOPIC ANALYSIS OF THE ADSORBENT

Fig. 5.1 shows the microscopic view of the duckweed plant

Fig:5.1 Microscopic images of the duckweed

5.2 MOISTURE CONTENT: Moisture content was determined by collecting 10g of *Lemna minor* and drying at 150°C and the amount of moisture content estimated was 86%. Fig. 5.2 depicts *Lemna minor* collected. The samples were separated into two groups: a training set was created to generate the calibration models, and a testing set was created to validate the models (Jin et.al. 2017). The water content in the training set ranged from 57.77 to 82.64%, whereas the water content in the testing set ranged from 58.20 to 85.94%, implying that the range of water content in the training set almost covered the

testing set (Jin et.al. 2017). Soil moisture had a substantial ($p < 0.05$) effect on plant height, stem diameter, number of leaves, and biomass. From week one through the last day of the experiment, all of the plants grew steadily in height (Chadha et.al.2019).

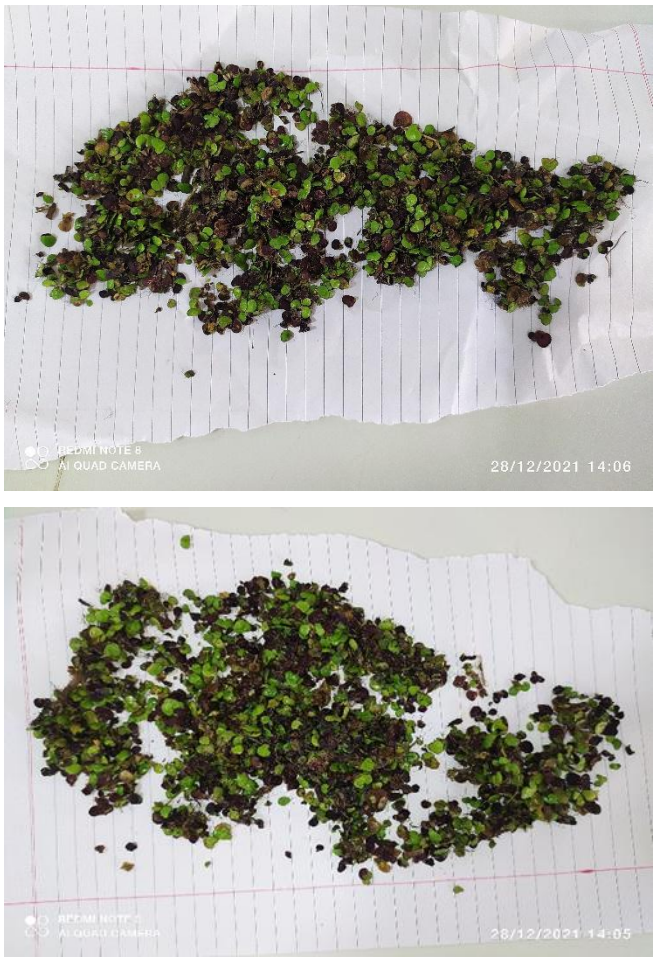

Fig. 5.2: Duckweed

Initial weight (W_1) – 10g

Weight after drying (W_2) – 1.4g

$$\text{Moisture content } (X_o) = \frac{W_1 - W_2}{W_1} \times 100 = \frac{10 - 1.4}{10} \times 100 = 86\%$$

5.3 PH DETERMINATION: pH was determined by dissolving 1g adsorbent in 100mL water followed by filtering the solution and determine the pH using digital pH meter. The pH value was estimated as 7.47. The initial pH of the solution is an important parameter since it determines plant surface charges and the degree of ionic strength (Can-Terzi et.al. 2021). The maximum pH range was therefore found to be 6.5–7.5, which was an ideal pH range for *L. minor* activity and growth (McLay 1976). The most critical variable influencing metal ion biosorption is solution pH (Lodeiro et.al. 2006; Hanif et.al. 2007). This is due in part to hydrogen ions' strong competition with metal ions. As a result of repulsive force, increased density of protons on the surface of biomass at low pH (pH 4) inhibited the approach of metal cations. At lower pH levels, more protons are available to protonate active groups of biomass surface, such as chitin, acidic polysaccharides, lipids, amino acids, and other plant cellular components, and metal ions compete with H^+ in the solution for adsorption (Sag, Kaya and Kutsal 1998) (Kaur, Gadgil and Sharma 2012).

5.4 POROSITY AND BULK DENSITY: The adsorbent (1g) was dispersed in 20ml water and centrifuged for 10min. Upon calculation, the porosity and bulk density was estimated as 80% & 6.25% respectively. The volumetric method results show that the percentage of vegetation porosity V_p in series I was 96, 92 and 88% for sparse, semi-dense and dense vegetation arrangements, respectively, and 92% in series II for all vegetation arrangements (Montakhab et.al. 2012). The greatest transpiration occurred at decreasing soil water potentials as the bulk density grew; the similar pattern was found for the potentials at which wilting occurred. As the bulk density grew, these variations were most likely caused by a decrease in aeration at high potentials and an increase in capillary conductivity at low potentials. The quantity of water extracted from the root zone rose with bulk density was due to the increase in capillary conductivity with rising density of the soil in the low capillary potential region (Yang and Jong 1971).

V_w – Volume of supernatant (water) = 16mL

V_T – Total volume of adsorbent = 20mL

M_a – Mass of adsorbent = 1g

$$\text{Porosity} = \frac{V_w}{V_T} = \frac{16}{20} = 0.8$$

$$R_{aw}\ (\text{Density}) = \frac{M_a}{V_w} = \frac{1}{16} = 0.0625\text{g/mL}$$

5.5 PORE VOLUME: Pore volume was calculated by dissolving 1g adsorbent in 10ml cylinder and boiling the sample in beaker with 20ml water followed by filtering, drying, and weighing. Fig. 5.3 depicts the pore volume of *Lemna minor* biomass whose volume was estimated to be 27.86mL. To quantify and explain the link between distinct pore sizes and pore volumes, the pore sizes against pore volume of *Lemna minor* was inferred from the soil water **r**etention **c**urves. The pore size categorization proposed in the literature (Greenland 1977) was changed based on the hydraulic function of the pores and the availability of biomass. Pore sizes responsible for water retention smaller than the **l**ower **l**imit were therefore classed as residual and bonding pores, those between the **l**ower **l**imit and **d**rained **u**pper **l**imit as storage pores, and those beyond the **d**rained **u**pper **l**imit as transmission pores. The pore volume and the amount of water that may be stored, known as plant-available water, are important features of storage pores. The volume of storage pores is determined by two important boundaries: the upper limit close to transmission pores, known as the DUL, and the upper limit of bonding or residual holes, known as the LL. Because various soils have varying DUL values, the assumption of pore classes for distinct types of soils in the fixed boundary classification appears undesirable and not scientifically justified (Mengistu, Mavimbela and Rensburg 2018).

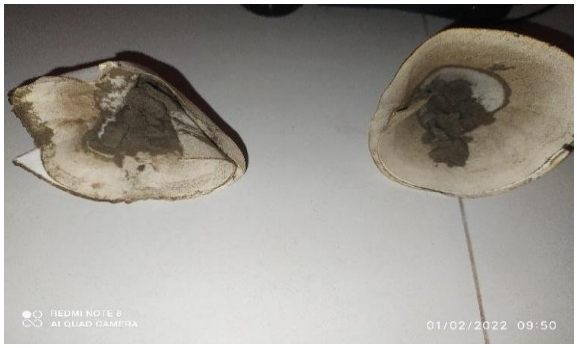

Fig: 5.3 Pore volume

Weight of Biomass 1 (W_1) = 1.705g

Weight of Biomass 2 (W_2) = 1.777g

Average increase in weight (W_I) = $\frac{W_1 + W_2}{2}$ = $\frac{1.705 + 1.777}{2}$ = 1.741g

Pore volume (V_P) = $\frac{W_I}{R_{aw}}$ = $\frac{1.741}{0.0625}$ = 27.856mL ~ 27.86mL

Table 5.1: Evaluation of Physical Properties

Substrate	Moisture content (g)	pH	Pore volume (mL)	Porosity (%)
Lemna minor adsorbent	0.9	7.5	28	80

5.6 PHYTOCHEMICAL ACTIVITY: In this study, Phytochemical analysis were undergone to identify phytochemical constituents of *L.minor* adsorbent. Fig. 5.4 depicts the phytochemical analysis of *Lemna minor* adsorbent. Table 5.2 interprets the results of phytochemical analysis where tannins, saponins, flavonoids, and terpenoids were present in *Lemna minor* adsorbent and phlobotannins, steroids and glycosides showed negative result. Each phytochemical demonstrated biological activity; for example, flavonoids have antioxidant potential (Savithramma, Rao and Suhrulatha 2011), alkaloids have antibacterial, analgesic and other antispasmodic properties (Savithramma, Rao and Suhrulatha 2011; Chatoui et.al. 2016; El Hattabi et.al. 2016), and steroids have anti-

inflammatory properties (Chatoui et.al. 2016). According to (Gordon, Stoops and Ratliff 1995; Sanjoaquin et.al. 2004; Topping and Clifton 2001; Lu 1993; P'ei and Chen 1982), plants include phytochemicals that have been isolated and are primarily employed to treat certain types of health-related problems, as well as in the production of nutritional supplements and minerals. Each phytochemical exhibits novel biological behaviour, which may increase the likelihood of the discovery of new compounds such as antibiotics against pathogens (Hassan and Ullah 2019; Sharifi-Rad 2016; Alghazeer et.al. 2012; Edziri et.al. 2010), and only flavonoids, which are polyphenols, play a role in antibiotic activity (Sato et.al. 2004; Cushnie and Lamb 2005) because flavonoids form complexes with bacterial proteins, cell walls, and other ingredients that are responsible for biological action (Cowan 1999). Many additional chemicals, such as terpenoids, tannins and saponins, also demonstrate antimicrobial (both bacterial and fungal) action in plants (Mamtha et.al. 2004) **(Hassan, Akmal and Nawaz 2020)**.

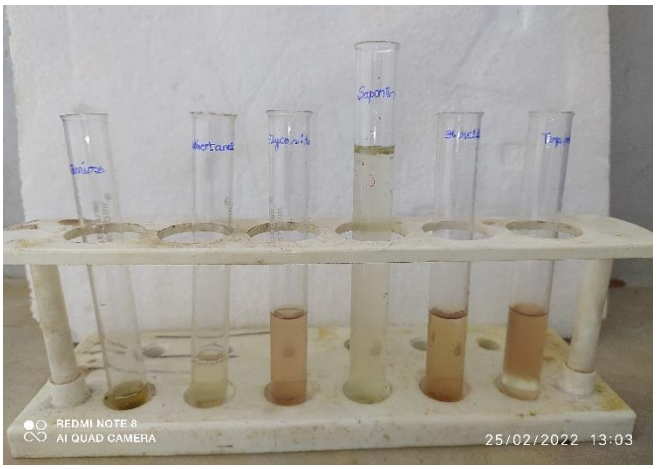

Fig: 5.4 Phytochemical analysis of Lemna minor adsorbent

Table 5.2: Results of Phytochemical analysis of *Lemna minor* adsorbent

Compound	Observation	Inference
Tannins	Presence of Brownish Green or Blue-Black Tint	+ve
Phlobatannis	Absence of red precipitate	–ve

Flavanoids	Presence of yellow colour	+ve
Saponin	Presence of emulsion	+ve
Steroids	Absence of green – violet to blue colour	–ve
Terpenoids	Presence of reddish-brown colour	+ve
Glycosides	Absence of brown ring	–ve

5.7 ELECTRICAL CONDUCTIVITY: Electrical conductivity was investigated by addition of 1g adsorbent in 100mL water and estimating the pH using EC meter. Fig. 5.5 depicts the EC meter whose measurement was estimated as **1.83S/m**. The experimental findings demonstrated that the designed EC sensing system worked effectively with nearly minimal variations between the targeted and observed EC values **(Othaman et.al. 2020)**. In the current study, EC was shown to have a significant reduction in control in the first 14 days of the trial. ANOVA analysis of one-way repeated measurements revealed that the concentration of EC in L. minor was not significantly different. However, the values of EC in control throughout the treatment period were significantly different. At the end of the trial, similar EC decreases were seen in A. filiculoides (69%) and L. minor (68%). Similarly, EC reductions after 21 and 28 days were not statistically different, suggesting that retention time beyond 21 days did not play a major role in EC elimination **(Amare, Kebede and Mulat 2018)**.

Fig: 5.5 Electrical Conductivity

5.8 PROTEIN ESTIMATION: Protein content was prepared by addition of 1g of duckweed powder in 100ml water followed by centrifuging, filtering and analysis using Lowry's technique presented in Table 5.3. Using Lowry's method, the average concentration of protein was estimated as 275µg/ml. The protein content of the material was approximately 34% on a dry weight basis, comparable to other duckweed varieties reported in the literature (Yu et.al. 2011) and significantly higher than the protein content of other leaf sources used for protein isolation, such as spinach (28% protein content on a dry basis) and lettuce (25% protein content on a dry basis), (Nations, [FAO] 1970) and significantly higher than the protein content of sugar beet leaves, which is 18% (CVB Veevoedertabel 2019). Using proteomics analysis, the proteins contained in the raw material include over 50% RuBisCO. Photosystem proteins, additional enzymes (such as ATP synthase and glutamine synthase), and ribosomal proteins are also detected in the raw duckweed material (Nieuwland et.al. 2021).

Table 5.3 Protein Estimation

Sample	Concentration µg/ml	Absorbance at 620 nm
A	100	0.093

B	200	0.010
C	300	0.052
D	400	0.094
E	500	0.041
DW T1	270	0.022
DW T2	280	0.023
	AVG: 275	

5.9 INITIAL CONCENTRATION AND THE ABSORBANCE OF THE METHYL ORANGE DYE: This was estimated by preparing 1000ppm of Methyl Orange dye (1g in 1000mL) and estimating the absorbance at 464nm using UV-spectrophotometer. Fig.5.6 illustrates the initial concentration and Fig.5.7 illustrates the absorbance of Methyl Orange Dye. Table 5.4 presents the values between Initial Concentration and the Absorbance of the Methyl Orange Dye at 464nm and Fig.5.7 represents the graph corresponding to Table 5.4. The influence of initial dye concentration on plant development was investigated, as well as dye uptake capability, until equilibrium was attained. Along with the nutrients, the plant was added to the colouring solution. For the sake of the investigation, the experiment was carried out at a pH of 7 using 1g of adsorbent (Reema et.al.2011). When the biosorption kinetics of Methyl Orange were tested at various initial concentrations, it was discovered that increasing the initial concentration (from 100 to 2000ppm) resulted in an increase in the biosorption capacity of *Lemna minor* (Prakash et.al. 2021). Increasing the initial dye concentrations causes the driving force to build in order to

overcome the resistance of dye mass transfer between the solution and the adsorbent surface, resulting in increased dye adsorption (Zazouli, Balarak and Mahdavi 2014) (Balarak, Mahdavi and Joghataei 2015).

Fig: 5.6 Initial Concentration

Table 5.4: Initial Concentration and the Absorbance of the Methyl Orange Dye

Concentrations (in ppm)	Absorbance at 464nm
100	0.29
200	0.389
300	0.407
400	0.447
500	0.512
600	0.536

700	0.679
800	0.692
900	0.737
1000	0.898
1100	0.913
1200	0.972
1300	1.05
1400	1.14
1500	1.155
1600	1.212
1700	1.235
1800	1.249
1900	1.354
2000	1.395

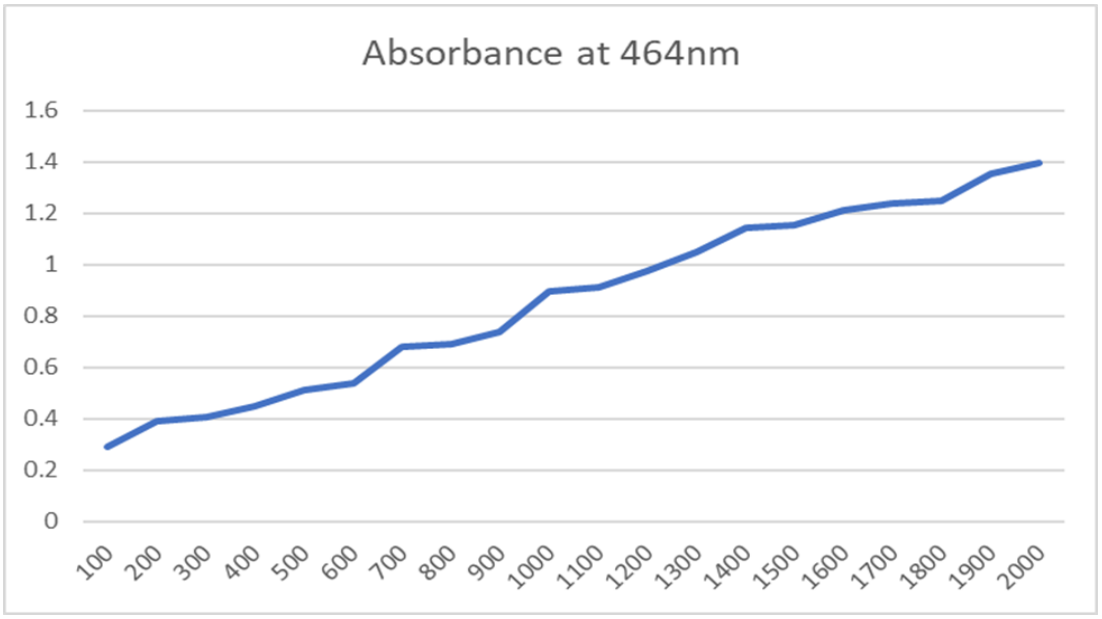

Fig: 5.7 Absorbance of dye at 464nm

5.10 DYE DEGRADATION: UV measurements were recorded at 464nm for three consecutive days at varying concentrations (100ppm to 2000ppm) of the dye solution containing 1g of substrate. After taking an average of the percentage removal for two consecutive days, it was discovered that at 1500ppm, the percentage removal of the methyl orange dye was greater. Fig. 5.8 shows the methyl orange dye solution following duckweed therapy on the 1st, 2nd and 3rd day. Table 5.5 illustrates the average % elimination of methyl orange dye over two days calculated by determining the dye concentration at various values and Fig.5.9 illustrates the graph corresponding to Table 5.5. Table 5.5 demonstrated that the methyl orange dye adsorption was greatest at 1500ppm. It was discovered that duckweed eliminated 91.7% of the methyl orange dye. When the day 3 samples were heated, it was discovered that desorption had occurred and the colour was darker than on day 1. As a result, it was demonstrated that the dye was absorbed.

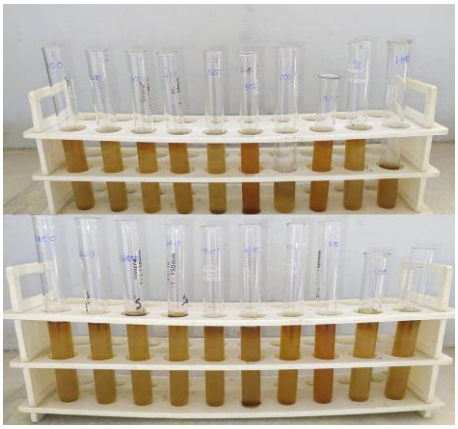

(a)

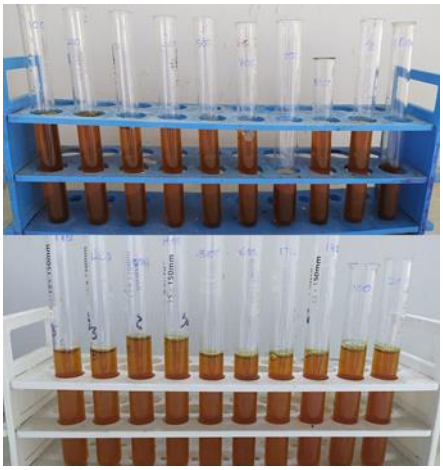

(b)

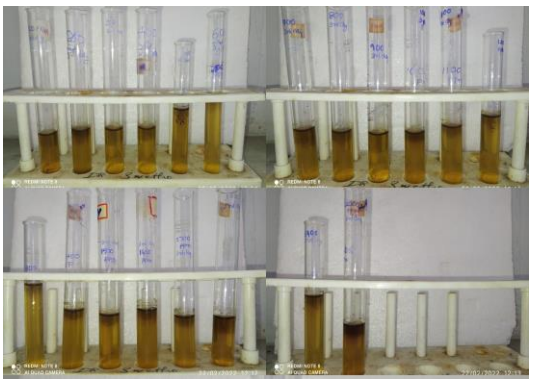

(c)

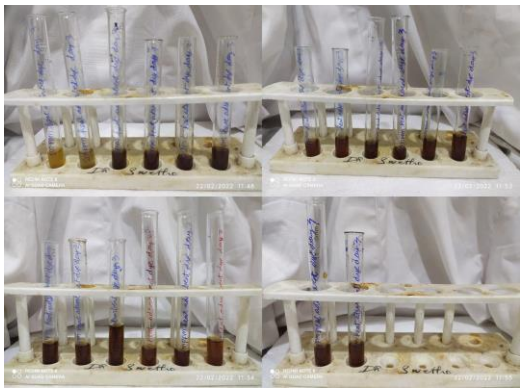

(d)

Fig: 5.8 Filtered extract of methyl orange dye treated by duckweed of 100ppm to 2000ppm concentrations (a) 1st day (b) 2nd day (c) 3rd Day (d) Desorption on 3rd day

Table 5.5: Percentage removal of methyl orange dye

Conc. (in ppm)	Abs. 464nm	Abs. 464nm Day 1	Abs. 464nm Day 2	Abs. 464nm Day 3	Day 1	Day 2	Day 3	% Day 1	% Day 2	% Day 3	Average
100	0.29	0.101	0.068	0.057	34.83	23.45	19.66	65.17	76.55	80.34	74.02
200	0.389	0.117	0.109	0.066	60.15	56.04	33.93	69.92	71.98	83.03	74.98
300	0.407	0.098	0.082	0.045	72.24	60.44	33.17	75.92	79.85	88.94	81.57
400	0.447	0.102	0.128	0.051	91.28	114.54	45.64	77.18	71.36	88.59	79.05
500	0.512	0.095	0.087	0.061	92.77	84.96	59.57	81.45	83.01	88.09	84.18
600	0.536	0.11	0.191	0.06	123.13	213.81	67.16	79.48	64.37	88.81	77.55
700	0.679	0.118	0.06	0.064	121.65	61.86	65.98	82.62	91.16	90.57	88.12
800	0.692	0.111	0.148	0.067	128.32	171.10	77.46	83.96	78.61	90.32	84.30
900	0.737	0.158	0.112	0.06	192.94	136.77	73.27	78.56	84.80	91.86	85.07
1000	0.898	0.113	0.179	0.057	125.84	199.33	63.47	87.42	80.07	93.65	87.05
1100	0.913	0.134	0.126	0.07	161.45	151.81	84.34	85.32	86.20	92.33	87.95
1200	0.972	0.109	0.079	0.07	134.57	97.53	86.42	88.79	91.87	92.80	91.15
1300	1.05	0.149	0.112	0.069	184.48	138.67	85.43	85.81	89.33	93.43	89.52

1400	1.14	0.159	0.106	0.095	195.26	130.18	116.67	86.05	90.70	91.67	89.47
1500	1.155	0.168	0.054	0.066	218.18	70.13	85.71	85.45	95.32	94.29	91.69
1600	1.212	0.164	0.136	0.091	216.50	179.54	120.13	86.47	88.78	92.49	89.25
1700	1.235	0.195	0.148	0.074	268.42	203.72	101.86	84.21	88.02	94.01	88.74
1800	1.249	0.24	0.169	0.082	345.88	243.55	118.17	80.78	86.47	93.43	86.90
1900	1.354	0.218	0.096	0.071	305.91	134.71	99.63	83.90	92.91	94.76	90.52
2000	1.395	0.251	0.084	0.098	359.86	120.43	140.50	82.01	93.98	92.97	89.65

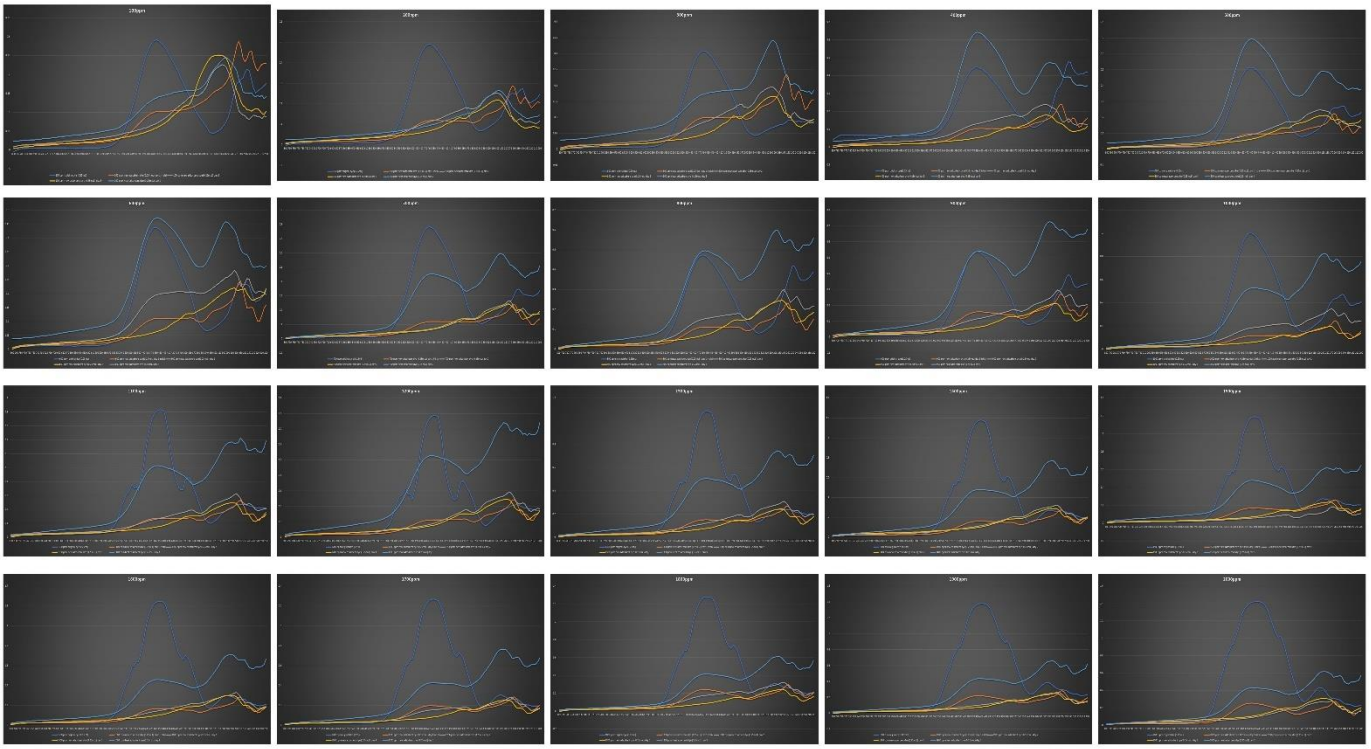

Fig:5.9 Dye Degradation from 100ppm–2000ppm

5.11 LACCASE ACTIVITY: The ABTS test was used to determine laccase activity. Laccase activity was measured to see if the dye was degraded. Laccase activity increased as the period of dye treatment with duckweed increased, as seen in Table 5.6 and Fig.5.10. Pollutants may be degraded by the metabolic process done by plant enzymes when exposed with plants (Aubert and Schwitzgue'bel 2004).

Table 5.6: Laccase activity of the day 2 and 3 extract after the treatment with duckweed

Conc.	Abs. 420nm	Vol. rxn mix	Dil. factor	Molar extinction coefficient	Vol. enzyme in rxn mix.	Incubation time	Result
2nd day							
100 ppm	0.199	3.25	12	36000	0.25	1	0.0008620
200 ppm	0.203	3.25	12	36000	0.25	1	0.0008800
300 ppm	0.169	3.25	12	36000	0.25	1	0.0007320
400 ppm	0.246	3.25	12	36000	0.25	1	0.0010660
500 ppm	0.204	3.25	12	36000	0.25	1	0.0008840
600 ppm	0.229	3.25	12	36000	0.25	1	0.0009920
700 ppm	0.264	3.25	12	36000	0.25	1	0.0011440
800 ppm	0.201	3.25	12	36000	0.25	1	0.0008710
900 ppm	0.021	3.25	12	36000	0.25	1	0.0000910
1000 ppm	0.299	3.25	12	36000	0.25	1	0.0012960
1100 ppm	0.25	3.25	12	36000	0.25	1	0.0010830
1200 ppm	0.165	3.25	12	36000	0.25	1	0.0007150
1300 ppm	0.278	3.25	12	36000	0.25	1	0.0012050
1400 ppm	0.298	3.25	12	36000	0.25	1	0.0012910
1500 ppm	0.311	3.25	12	36000	0.25	1	0.0013480
1600 ppm	0.326	3.25	12	36000	0.25	1	0.0014130
1700 ppm	0.252	3.25	12	36000	0.25	1	0.0010920
1800 ppm	0.355	3.25	12	36000	0.25	1	0.0015380
1900 ppm	0.253	3.25	12	36000	0.25	1	0.0010960
2000 ppm	0.24	3.25	12	36000	0.25	1	0.0010400
Control	0.016	3.25	12	36000	0.25	1	0.0000693
3rd day							
100 ppm	0.438	3.25	12	36000	0.25	1	0.001898
200 ppm	0.254	3.25	12	36000	0.25	1	0.001101
300 ppm	0.273	3.25	12	36000	0.25	1	0.001183
400 ppm	0.452	3.25	12	36000	0.25	1	0.001959
500 ppm	0.196	3.25	12	36000	0.25	1	0.000849

600 ppm	0.209	3.25	12	36000	0.25	1	0.000906
700 ppm	0.365	3.25	12	36000	0.25	1	0.001582
800 ppm	0.448	3.25	12	36000	0.25	1	0.001941
900 ppm	0.329	3.25	12	36000	0.25	1	0.001426
1000 ppm	0.386	3.25	12	36000	0.25	1	0.001673
1100 ppm	0.294	3.25	12	36000	0.25	1	0.001274
1200 ppm	0.255	3.25	12	36000	0.25	1	0.001105
1300 ppm	0.289	3.25	12	36000	0.25	1	0.001252
1400 ppm	0.37	3.25	12	36000	0.25	1	0.001603
1500 ppm	0.486	3.25	12	36000	0.25	1	0.002106
1600 ppm	0.477	3.25	12	36000	0.25	1	0.002067
1700 ppm	0.411	3.25	12	36000	0.25	1	0.001781
1800 ppm	1.189	3.25	12	36000	0.25	1	0.005152
1900 ppm	0.391	3.25	12	36000	0.25	1	0.001694
2000 ppm	0.435	3.25	12	36000	0.25	1	0.001885
Control	0.068	3.25	12	36000	0.25	1	0.000295

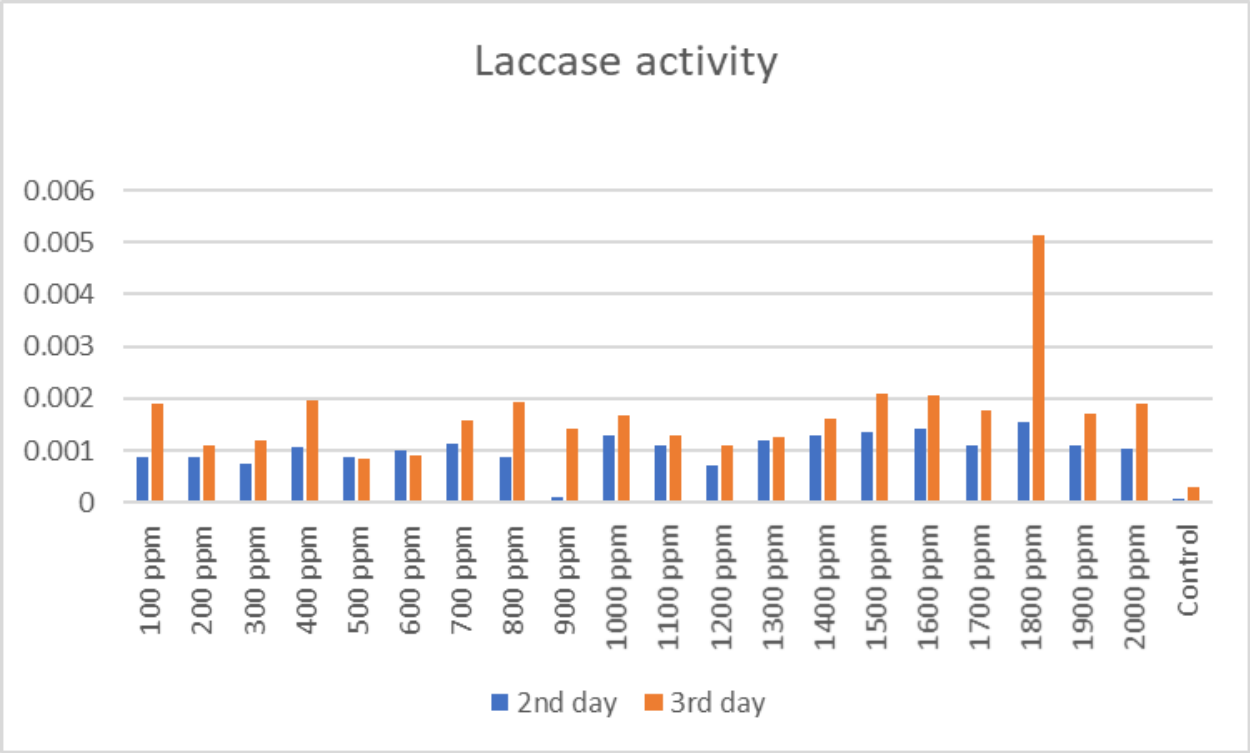

Fig:5.10 Graphical representation of laccase activity

5.12 DYE DECOLORIZATION: The absorbance of 1500ppm methyl orange dye was determined for different time intervals (0th hour, 24th hour, 48th hour, 72nd hour) (Fig. 5.11 & 5.13) and it was discovered that as time passed, the absorbance dropped (Fig. 5.12). As a result, it was demonstrated that it had enhanced absorption (Table 5.7). The absorption capability of duckweed obtained in this investigation was consistent with the literature (Reema et.al. 2011). According to Reema et al. (2011), increasing dye concentration (2, 4, 6, 8, and 10mg/L) enhanced the efficiency of Methyl Orange removal due to increase in the absorption capacity of *L. minor* with rising concentration gradient and driving force for the biosorption capacity. Methyl Orange (91%) was identified in wild plants such as *S. molesta*, *Ipomoea hederifolia*, *F. dichtomas*, and *Asparagus densiflorus* within 72, 60, 60, and 48 hours, respectively (Chandanshive et.al. 2020)

(a)

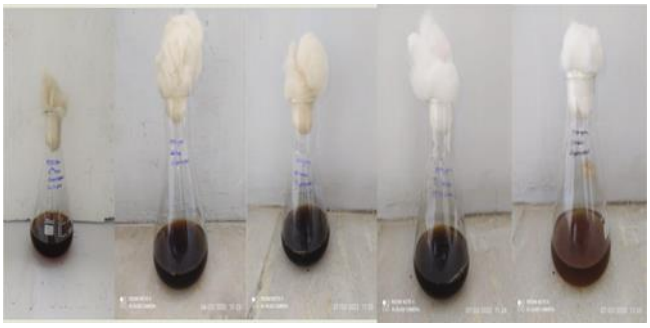

(b)

Fig:5.11: Methyl orange dye (1500 ppm) at different intervals (a) before treatment

(b) After treatment

Table 5.7 Dye Decolorization

Concentration	Time	Wavelength	Absorbance
1500 ppm	0^{th} Hour	464 nm	0.519
1500 ppm	24^{th} Hour	464 nm	0.349
1500 ppm	48^{th} Hour	464 nm	0.27
1500 ppm	72^{nd} Hour	464 nm	0.26
Control	72^{nd} Hour	464 nm	0.082

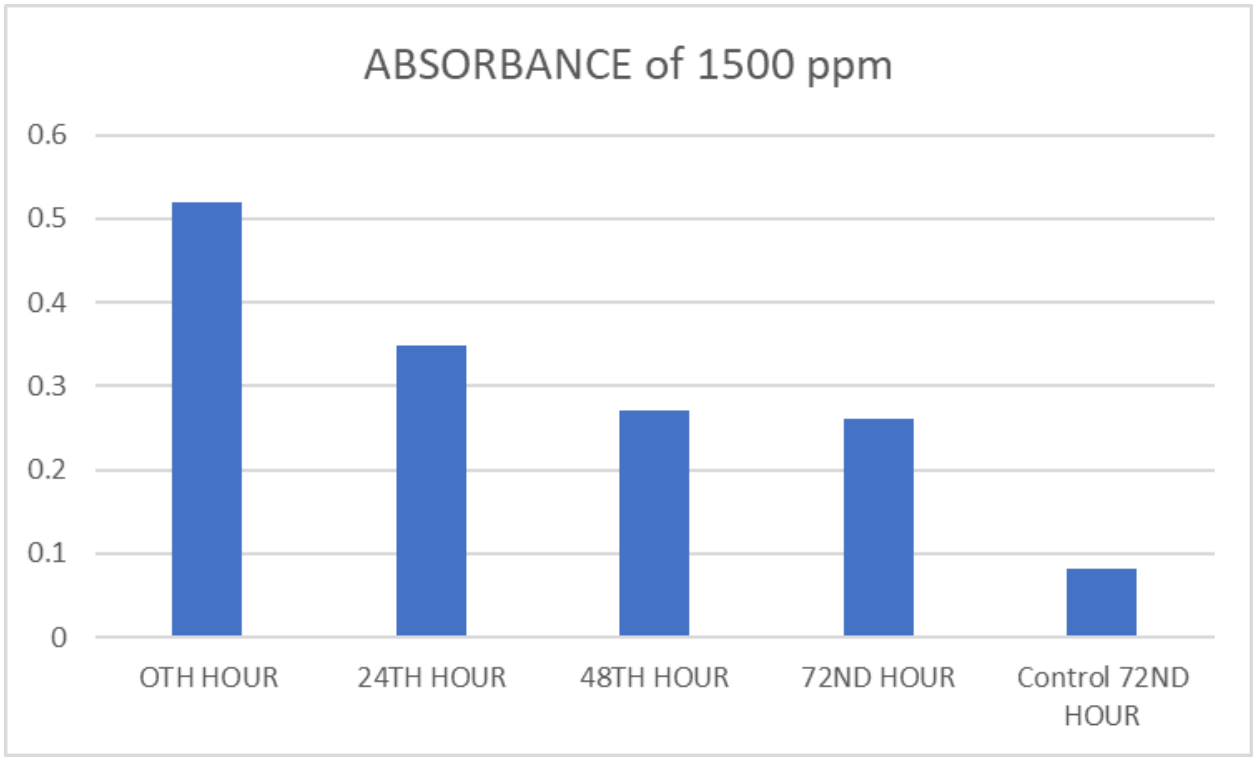

Fig: 5.12 Graphical representation of 1500ppm concentration and it's absorbance at different intervals

(a)

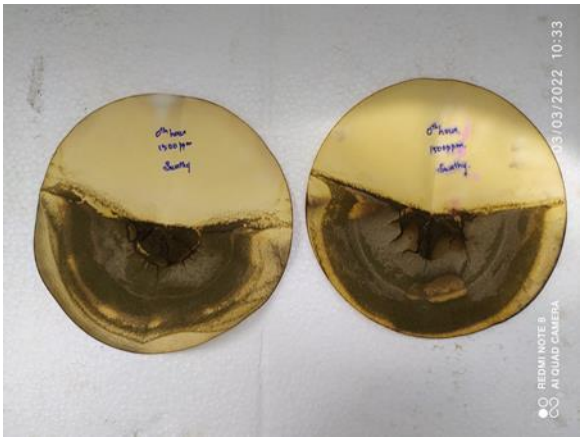
05/03/2022 10:33
REDMI NOTE 8
AI QUAD CAMERA

(b)

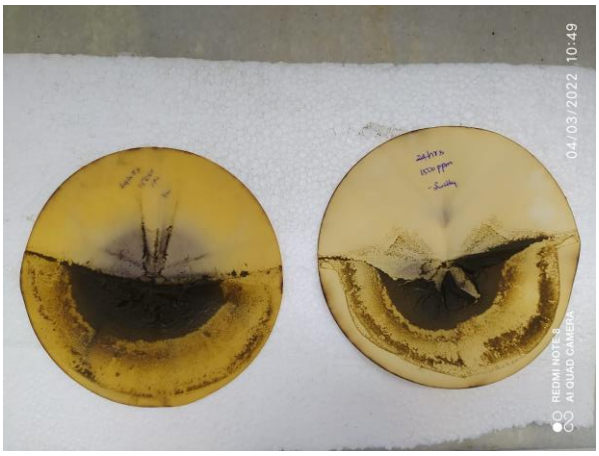
04/03/2022 10:49
REDMI NOTE 8
AI QUAD CAMERA

(c)


05/03/2022 13:26
REDMI NOTE 8
AI QUAD CAMERA

(d)

(e)

Fig: 5.13: Filtered treated adsorbent of 1500 ppm at different time intervals, (a) Control (b) 0th hour c) 24th hour d) 48th hour e) 72nd hour

5.13 MICROBIAL ANALYSIS: MH agar was used for microbial analysis. It revealed that there was no microbial growth in the Aqueous duckweed, 48th hour, and control samples. As a result, it was established that there was no interaction between microorganisms and duckweed and methyl orange dye adsorption (Fig. 5.14).

Fig: 5.14: Extract Before and after incubation for microbial growth

5.14 PARAMETERS OPTIMIZATION:

5.14.1 Effect of Temperature: 0.25g of *Lemna minor* was combined with 25ml of distilled water containing 1500ppm of methyl orange colour. Optimization of Temperature was carried out in different factors and at different time intervals illustrated in Table 5.8 and Fig. 5.14a represents the graph of Table 5.8. It was discovered that when the temperature rose, the absorbance and laccase activity dropped. This may be due to increasing the mobility of the dye molecules and an increase in the number of active sites for the adsorption with increasing temperature (Wang et.al. 2005; Mall et.al. 2006) (Balarak et.al. 2016).

Table 5.8 Optimization of Temperature

Temp.	**Room Temp.**				**Boiled**				**Cooled**			
Time	**Absorbance**		**Laccase**		**Absorbance**		**Laccase**		**Absorbance**		**Laccase**	
	Treat	Control	Treat	Control	Treat	Control	Treat	Control	Treat	Control	Treat	Control
0^{th} hour	0.692	0.067	0.617	0.144	0.757	0.075	0.873	0.14	0.722	0.12	1.014	0.173
3^{rd} hour	0.661	0.022	0.526	0.124	0.476	0.091	0.416	0.132	0.401	0.097	0.483	0.158
6^{th} hour	0.600	0.010	0.666	0.100	0.389	0.132	0.546	0.134	0.357	0.096	3.000	0.063

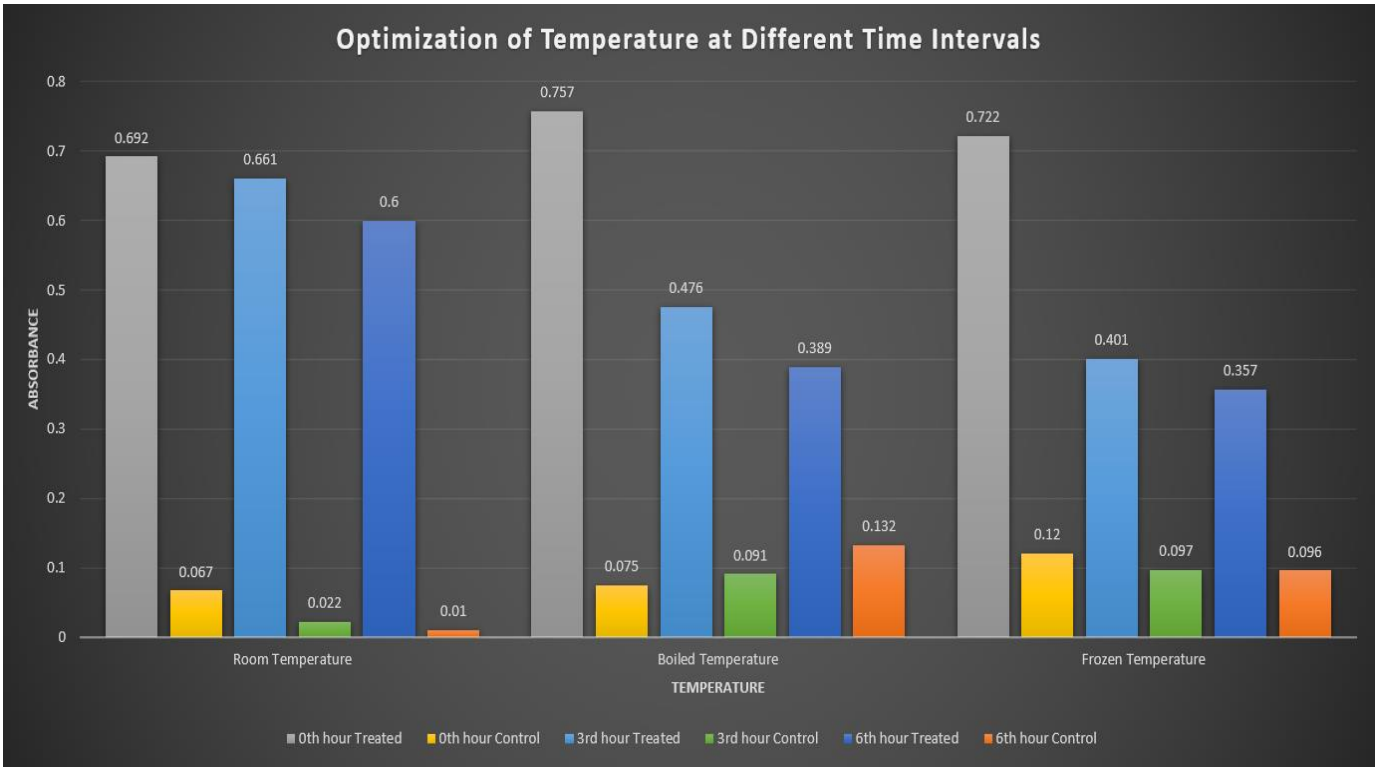

Fig:5.15 Optimization of Temperature for Control and Adsorbent Biomass at different time intervals

5.14.2 Effect of pH: For the Control and Adsorbent at the concentration of 1500ppm, the pH values ranging from 4–7 was set in different time intervals. The values of pH at different time intervals is illustrated in Table 5.9 and graph is illustrated in Fig.5.15b. To achieve the increased adsorption dye capacity, parameter tuning is required. The pH of the solution is critical in influencing the entire adsorption process. Because of the external adsorbent morphological character and different ionic form of the dyes, an increased removal of 98.9% was achieved at pH 4, where the process significantly depletes as pH increases and is represented in. At pH values ranging from 4.0 to 6.0, dye molecules acquire a negative sulfonate group, resulting in a significant electrostatic interaction between sulfonate and proton molecules on the sorbent surface. The presence of proton molecules on the sorbent surface affects the structure and arrangement of dye molecules (Lee et.al. 2016). The presence of a negative charge on the surface of the adsorbent that attracts the dye molecule decreases its attraction **(Prakash et.al. 2021)**.

Table 5.9: Optimization of pH

pH	4				5				6				7			
Time	Abs.		Laccase		Abs.		Laccase		Abs.		Laccase		Abs.		Laccase	
	T	C	T	C	T	C	T	C	T	C	T	C	T	C	T	C
0th hour	0.655	0.014	0.43	0.22	0.575	0.051	0.425	0.128	1.092	0.057	0.581	0.126	0.88	0.07	0.555	0.129
6th hour	0.295	0.074	0.309	0.144	0.371	0.121	0.355	0.157	0.46	0.104	0.437	0.181	0.447	0.117	0.437	0.152

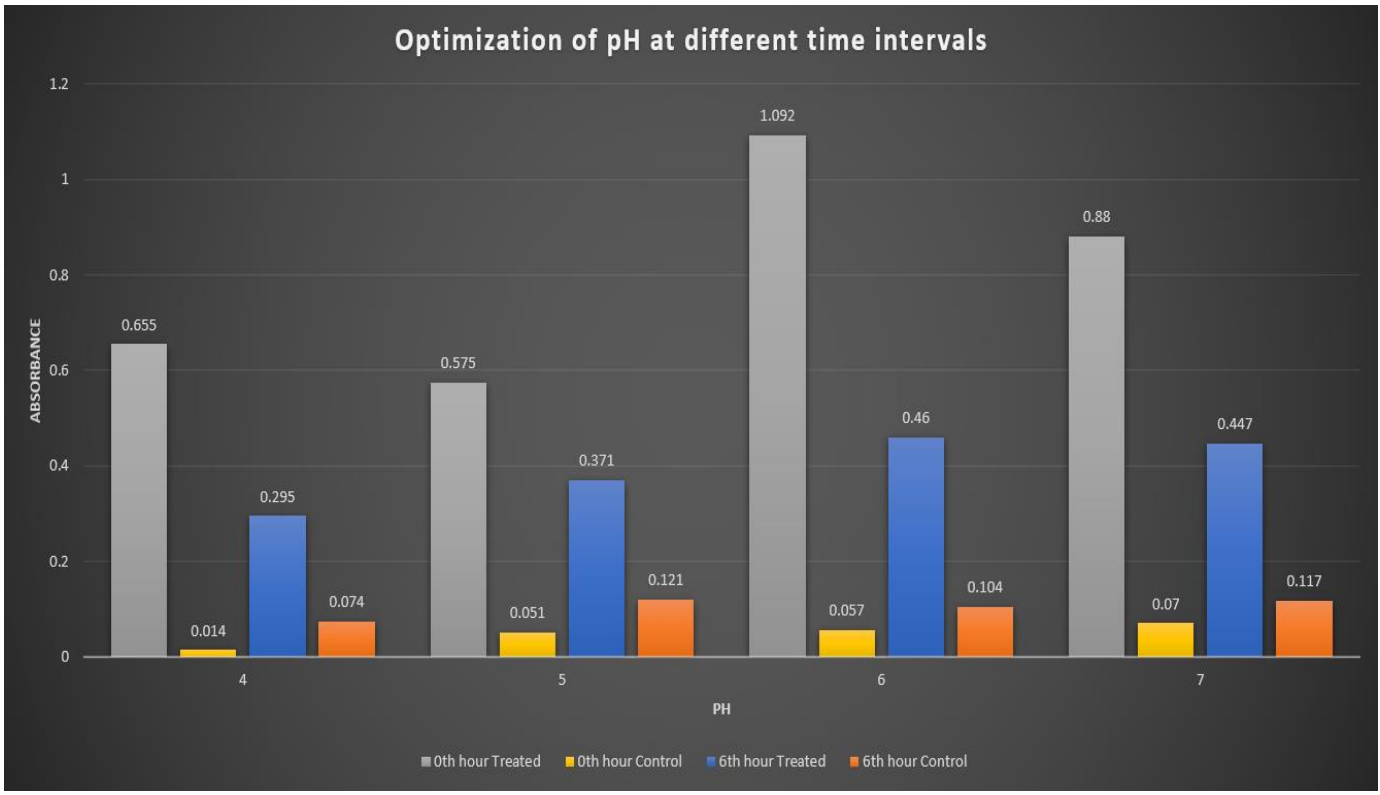

Fig:5.16 Optimization of pH for Control and Adsorbent Biomass at different time intervals

5.15 ISOTHERM STUDIES

Isotherm: Various isotherm approaches, such as Langmuir, Freundlich, Langmuir–Freundlich, and Temkin expressions, were used to explain the dye-binding process with the adsorbent. The current study proposed varied dye

concentrations ranging from 100 – 1500ppm at pH 7, temperature 35°C, and an equilibrium contact period of 6min. Among the parameters analyzed, Temkin isotherm was the best fitting isotherm illustrated in Table 5.10 and Fig.5.15c illustrates the graph corresponding to Table 5.10.

Table 5.15: Temkin Isotherm Model

Time	100	200	300	400	500	600	700	800	900	1000	1100	1200	1300	1400	1500
0	99	98.9	97.3	99.3	96.6	99.6	99.2	98.6	98.7	99.5	98.7	97.9	98.4	97.7	97.1
6	87	86.8	87.1	86.2	85.5	85.9	84.8	85.4	85.1	84.7	84.5	84.6	83.8	83.7	82.3
12	79.6	79.4	79.3	78.9	78.6	78.4	77.8	77.5	77.2	76.7	76.8	76.6	76.1	75.4	75.2
18	66.9	66.5	65.7	65.4	65.2	65	65.1	64.8	64.7	64.5	63.6	63.3	62.9	62.5	62.3
24	58	57.7	57.4	57.3	56.9	56.8	56.4	56.1	55.8	55.5	55.4	55	54.7	54.2	54.1
30	46.8	45.8	45.8	45.6	45.4	45.3	45	44.9	45.1	44.8	44. 5	44.2	44.3	43.7	43.5
36	43.2	43.9	42.6	42.7	42.5	42	41.8	41.6	41.3	41.2	40.7	40.5	40.4	40.1	40
42	38.9	38.6	38.5	38.4	38.3	38.2	38.1	38	37.9	37.7	37.4	37.3	36.9	36.8	36.3
48	27	26.8	26.7	26.5	26.4	26.3	26.1	26	25.9	25.7	25.5	25	24.8	24.3	24
54	25.9	25.8	25.5	25.3	25	24.8	24.6	24.4	24.2	24	24.1	23.9	23.6	23.3	23.2
60	19.3	19.1	19	19.1	18.8	18.8	18.6	18.5	18.4	17.7	17.4	17.1	16.7	16.5	16.2
66	15.7	15.5	15.4	15.6	15.3	14.7	14.6	14.8	14.3	13.7	13.5	13	12.8	12.3	12
72	0.5	1.3	1.9	2.4	3.2	3.8	4	4.3	4.5	4.7	5.2	5.3	6.4	6.5	6.6
Ce	0.5	1.3	1.9	2.4	3.2	3.8	4	4.3	4.5	4.7	5.2	5.3	6.4	6.5	6.6
Qe	9.85	19.52	28.62	38.76	46.7	57.48	66.64	75.44	84.78	94.8	102.85	111.12	119.6	127.68	135.75
1/Qe	0.101523	0.05123	0.034941	0.0258	0.021413	0.017397	0.015006	0.013256	0.011795	0.010549	0.009723	0.008999	0.008361	0.007832	0.007366
1/Ce	2	0.769231	0.526316	0.416667	0.3125	0.263158	0.25	0.232558	0.222222	0.212766	0.192308	0.188679	0.15625	0.153846	0.151515
ln Qe	2.287471	2.97144	3.354106	3.657389	3.843744	4.051437	4.199305	4.323338	4.44006	4.551769	4.633272	4.710611	4.784153	4.849527	4.910815
ln Ce	-0.69315	0.262364	0.641854	0.875469	1.163151	1.335001	1.386294	1.458615	1.504077	1.547563	1.648659	1.667707	1.856298	1.871802	1.88707

In Ce	Qe
-0.69315	9.85
0.262364	19.52
0.641854	28.62
0.875469	38.76
1.163151	46.7
1.335001	57.48

1.386294	66.64
1.458615	75.44
1.504077	84.78
1.547563	94.8
1.648659	102.85
1.667707	111.12
1.856298	119.6
1.871802	127.68
1.88707	135.75

B= $\frac{R_T}{b}$	Slope	9.21
B ln A	intercept	9.47
ln A		1.02823
A		2.796113

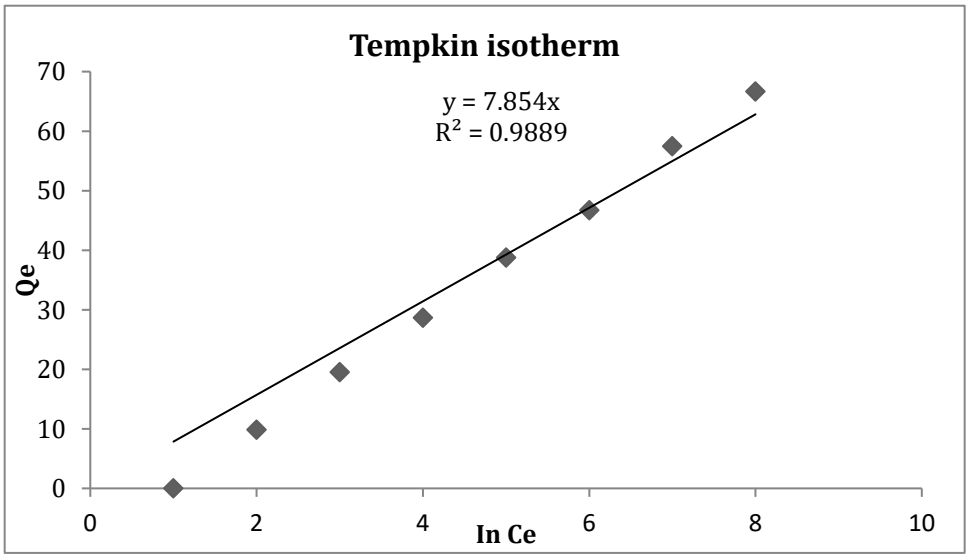

Fig: 5.17 Isotherm model (Temkin)

5.16 CHARACTERIZATION:

5.16.1 ***SEM:*** Scanning electron microscopy (SEM) was used to determine the surface morphology of the substrates. Duckweed and adsorbed duckweed surface morphology were studied. Fig. 5.16 – 5.18 shows the analysis of Powder, 72h adsorbent and Control Biomass done in different magnifications for clear understanding of the surface morphology of *Lemna minor* biomass which implied that the analysis indicated best organization and uniform porosity with large and irregular cavitations around *Lemna minor* providing large surface area for adsorption (Naghipour et.al. 2015). It reveals that the sorbent has a rough and porous character with an increased surface area, which promotes strong interaction with the Methyl Orange dye (Prakash et.al. 2021).

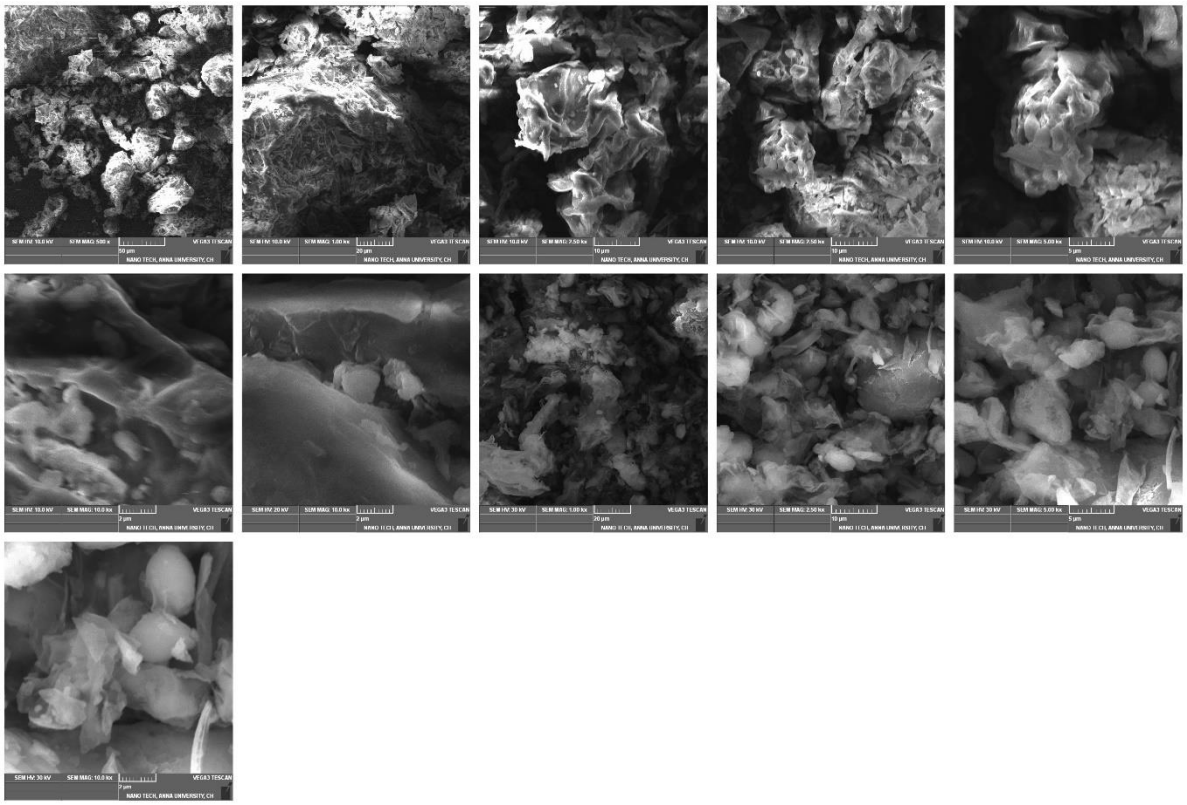

Fig: 5.18 SEM analysis of Powder taken at 500×, 1k×, 2.5k×, 5k× and 10k×

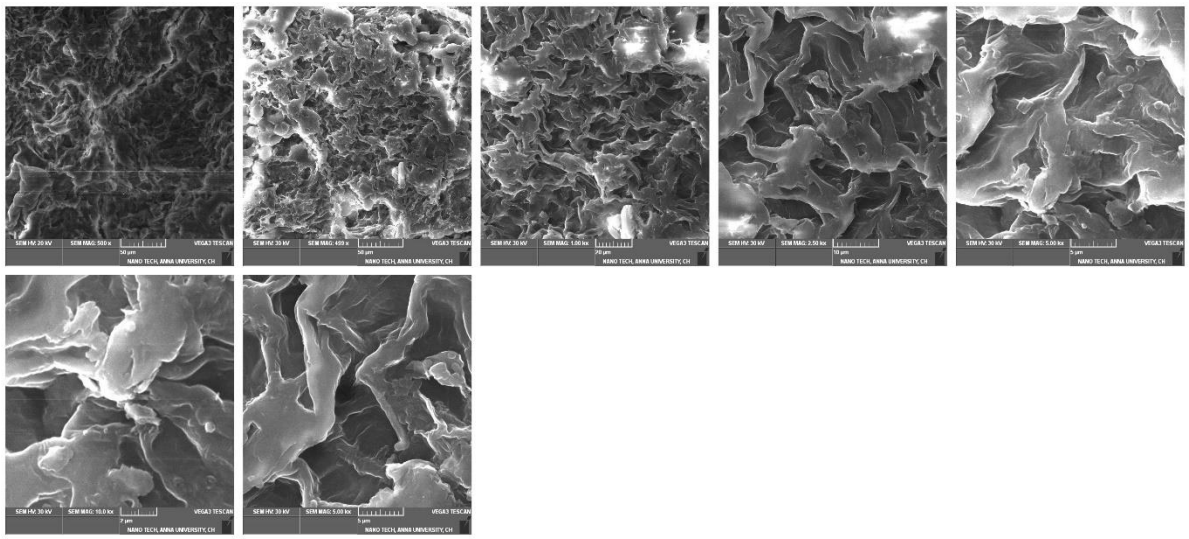

Fig: 5.19 SEM analysis of 72h adsorbent taken at 499×, 500×, 1k×, 2.5k×, 5k× and 10k×

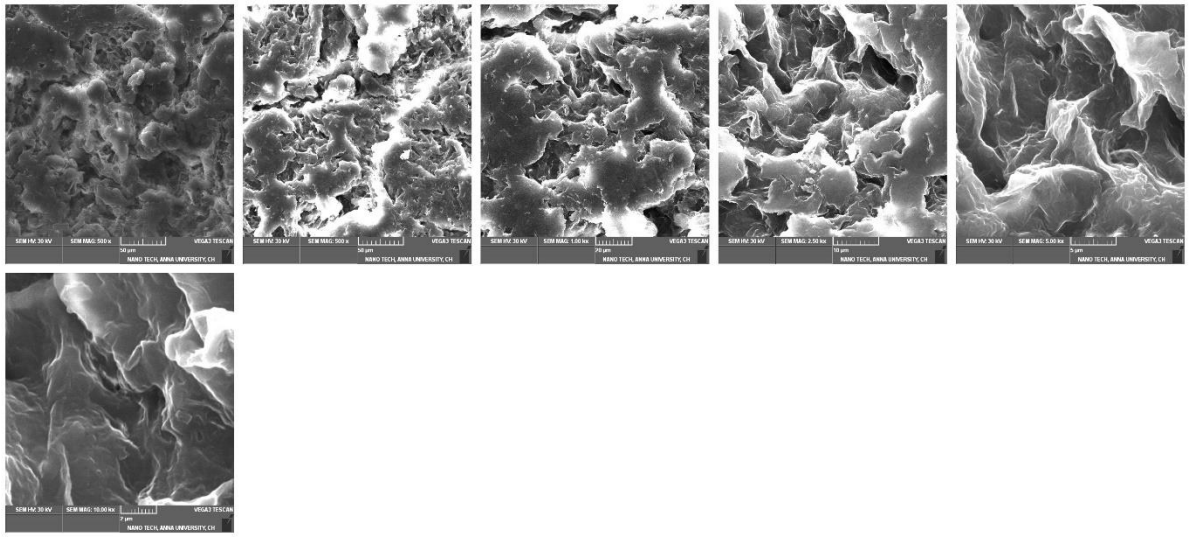

Fig: 5.20 SEM analysis of Control Biomass taken at 500×, 1k×, 2.5k×, 5k× and 10k×

5.16.2 ***FTIR:*** Fourier transform infrared (FTIR) is a technique that uses infrared radiation to produce spectra which enables identification and quantification of the compounds. Each peak corresponds to a particular functional group. By using this technique, the

functional groups that may be active in the substrate and play a role in adsorption and degradation can be identified. Fig. 5.19 – 5.21 depicts the FTIR analysis of Control Biomass, Methyl Orange dye and adsorbent from 0th hour to 72nd hour respectively implying that Lemna minor adsorbent exhibited Alcohol, Alkane, Sulphate, Phenol, Amine, Ether, Halo compounds, Carbon dioxide, Nitrile, Ester and Nitro compounds. As a result, the results showed that the Methyl Orange dye was used as a carbon and nitrogen source, as well as being integrated in plant functional groups. The FTIR results indicated that L. minor's Methyl Orange dye removal method was most probably biosorption (Can-Terzi et.al. 2021).

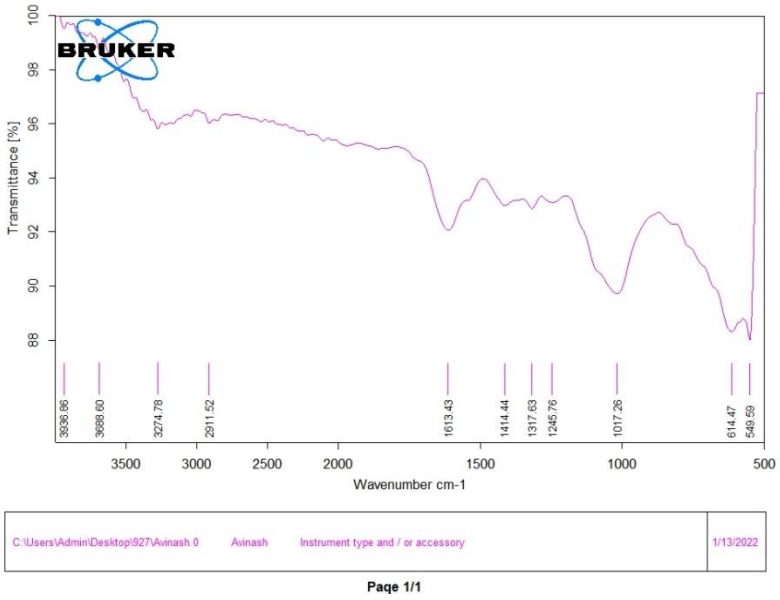

Fig: 5.21: FTIR Results of Control Biomass

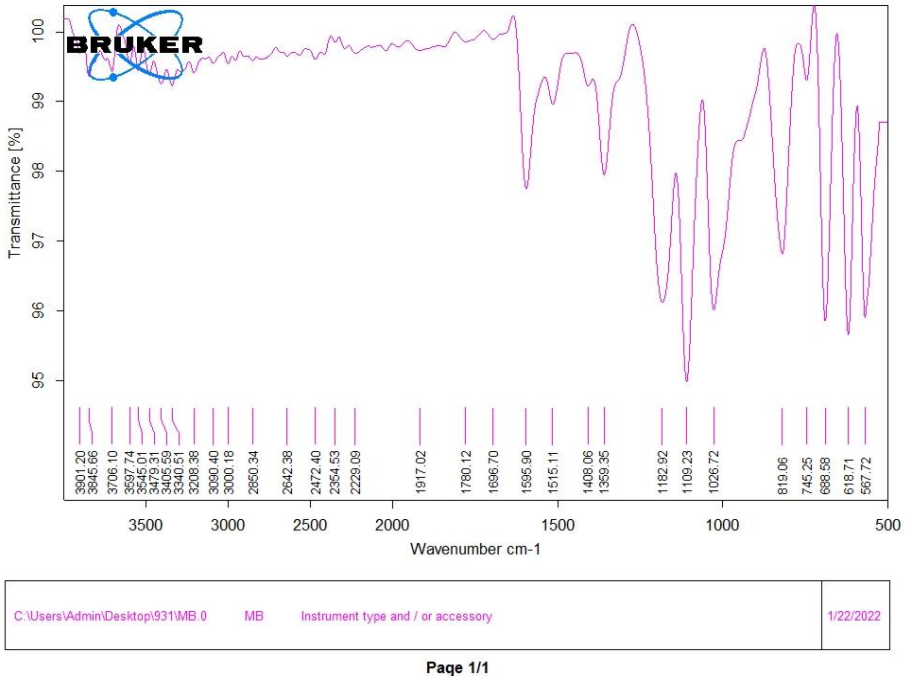

Fig: 5.22: FTIR Results of Methyl Orange

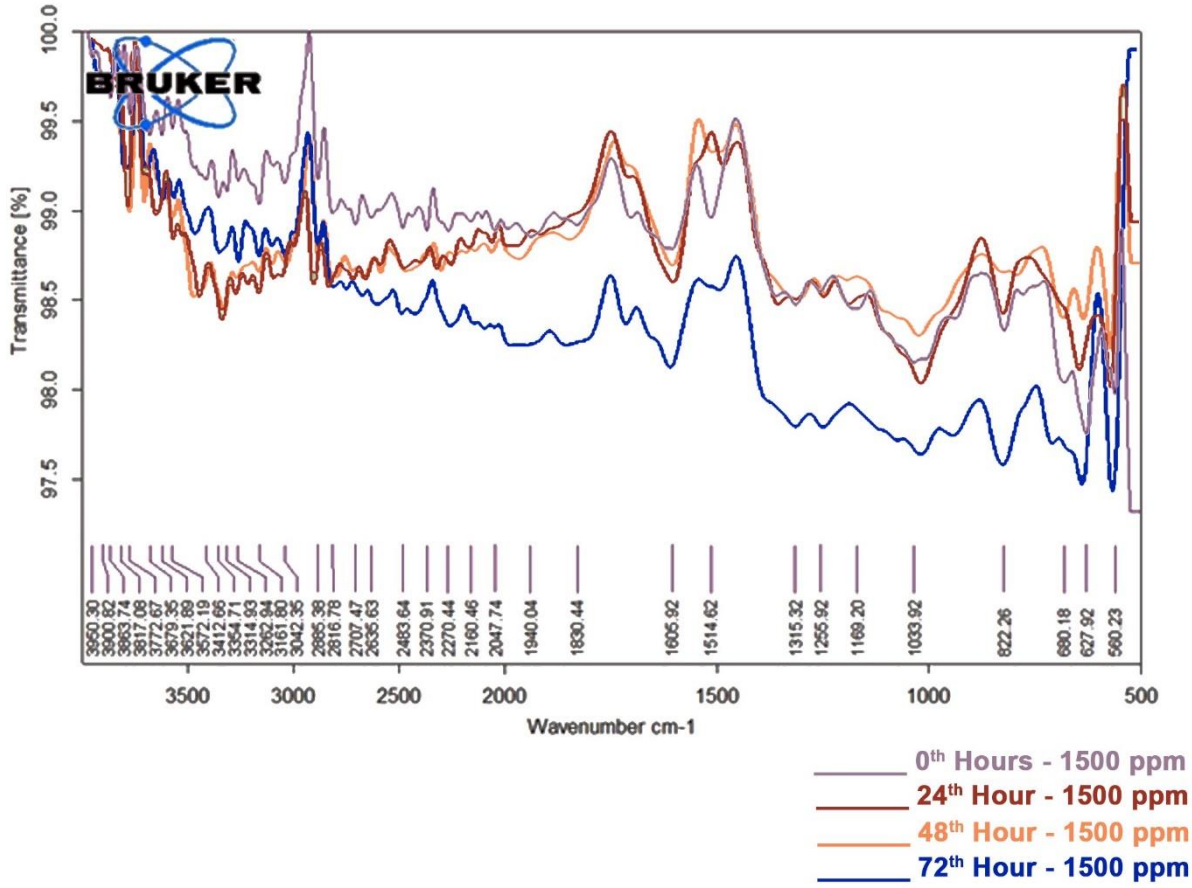

Fig: 5.23: FTIR Results of Adsorbent at 1500ppm concentration (0th Hour, 24th Hour, 48th Hour and 72nd Hour)

5.16.3 *GCMS:* GCMS separated chemical mixtures (the GC component) and identified the components at the molecular level (the MS component) as well as potential metabolites. GCMS was used to examine the dye solution after treatment as well as the effluent before and after treatment. Table 5.11 illustrates the bioactivity of the compounds measured in different Residual Time and different factors which implied that the adsorbent not only adsorbs the dye, but it could also degrade the aromatic dye molecules (Prakash et.al. 2021).

Table 5.10: GCMS analysis and the bioactivity of compounds

Residence Time	% Area	Compound Name	Structure	Bioactivity

0th hour adsorbent				
4.716	70.78	Diacetone alcohol	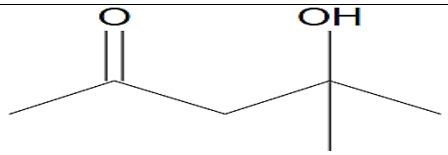	antimicrobial activity (*Seddek N.H. et.al.* 2019)
15.677	51.73	9-Hexadecenoic acid		Antioxidant activity (*Rahman M.M et.al.* 2014)
18.899	72.67	1-Hexadecene		Antimicrobial and Antioxidant Activities (*Mou Y. et.al.* 2013)
21.732	58.22	10-Henicosene		antimicrobial activity (*Vanitha V. et.al.* 2020)
23.695	32.09	Methyl palmitate		Antihelmintic and Antibacterial activity (*Adnan et.al.* 2019)
24.273	41.32	10-Henicosene		antimicrobial activity (*Vanitha V. et.al.* 2020)
25.847	98.43	16-octadecenoate	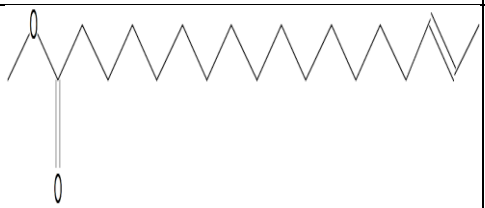	anti-inflammatory activities (*Silva R.O. et.al.* 2014, *Siswadi S. and Saragih G.S.* 2021)
26.682	37.36	2-Hexyldecanol	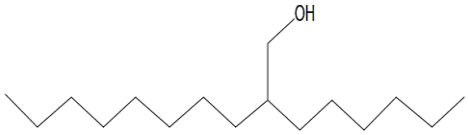	A regulator of ubiquitin–proteasome activity (*Hakozaki T. et.al.* 2013)
28.937	39.59	22-Hentriaconten-2-one		antitumor activity (*Kim S.J. et.al.* 2011, *Jaihyunk R. et.al.* 2020)
30.738	100.00	1,1,3,3,5,5,7,7,9,9,11,11,13,13,15,15-Hexadecamethyloctasiloxane	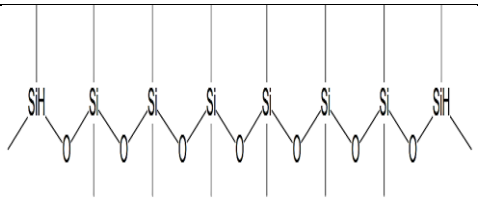	Antimicrobial activity (*Kumaradevan et.al.* 2015, *Boominathan M. and Bakiyalakshmi S.V.* 2016)

32.920	92.07	n-Tetracontane	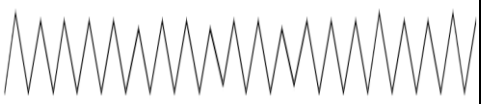	antimicrobial agent (*Kawuri R. and Darmayasa I.B.G.* 2019)
34.780	53.61	1,8,15,22-Tetraazacyclooctacosane-2,7,16,21-tetrone	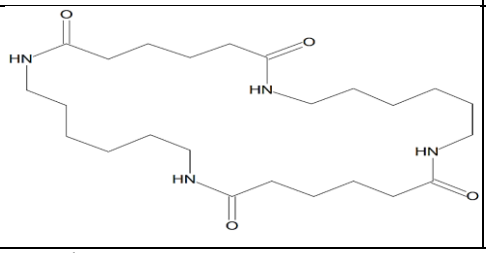	No activity reported
72nd hour adsorbent				
3.734	23.8	3,3-Diethylazetidin-2,4-dione	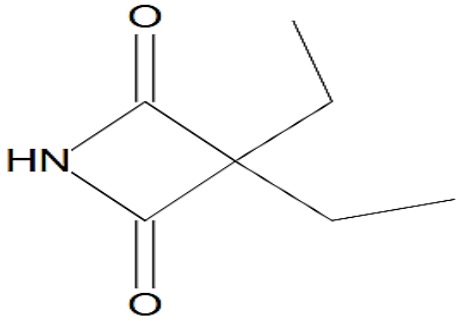	competitive GABA uptake inhibitor (*Sunday Otimenyin* 2022)
3.932	28.1	2,4-Dimethyl-2-pentene	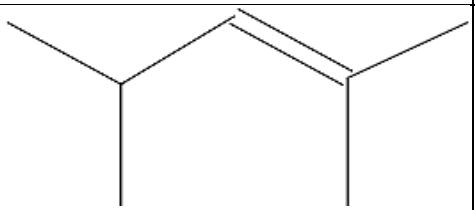	as a pesticide, as an additive to gasoline, and in the manufacture of other chemicals
4.512	74.5	Diacetone alcohol	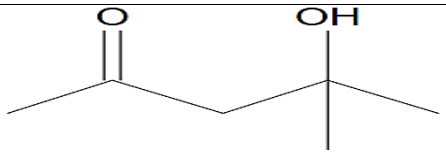	antimicrobial activity (*Seddek N.H. et.al.* 2019)
5.616	73.6	Diacetone alcohol	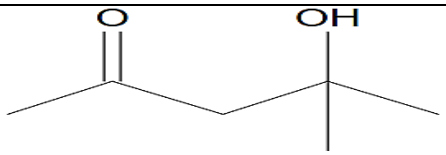	antimicrobial activity (*Seddek N.H. et.al.* 2019)
21.176	21.6	4-(1-(4-[1-(4-Hydroxyphenyl)-1-methylethyl]phenyl)-1-methylethyl)phenol	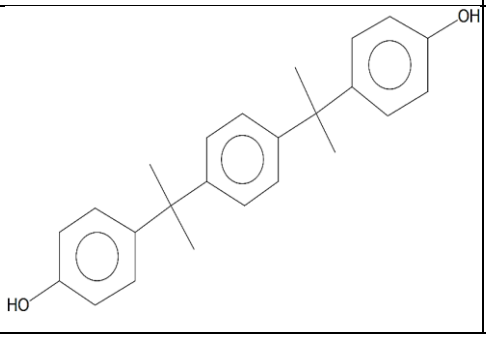	Estrogenic and Anti-estrogenic, Androgenic and Anti-androgenic, Thyroid and Anti-thyroid Activity

22.538	40.6	2,4,6-Triphenyl-1,3,5-tripropylborazine	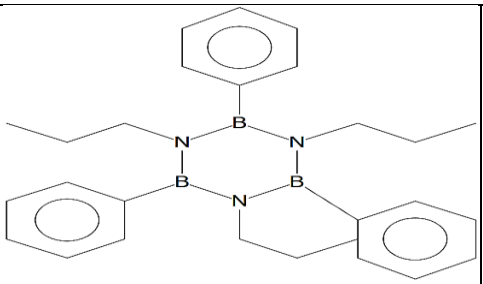	starting materials for boron carbonitrides
23.804	65.1	1,1,3,3,5,5,7,7,9,9,11,11,13,13,15,15-Hexadecamethyloctasiloxane	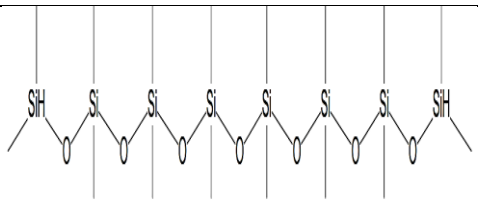	Antimicrobial activity (*Kumaradevan et.al.* 2015, *Boominathan M. and Bakiyalakshmi S.V.* 2016)
24.375	24.3	3,3'-Dimethoxy-N,N'-bis(p-methoxybenzylidene)benzidine	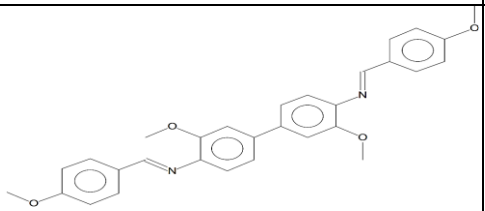	production of textiles, paints, printing inks, paper, and pharmaceuticals
25.715	40.6	1,1,3,3,5,5,7,7,9,9,11,11,13,13,15,15-Hexadecamethyloctasiloxane	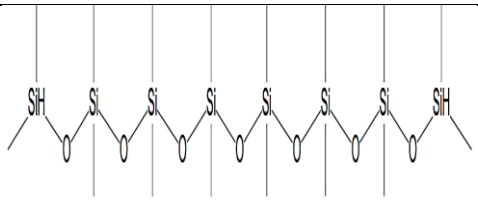	Antimicrobial activity (*Kumaradevan et.al.* 2015, *Boominathan M. and Bakiyalakshmi S.V.* 2016)
26.362	6.33	Chlorthalidone	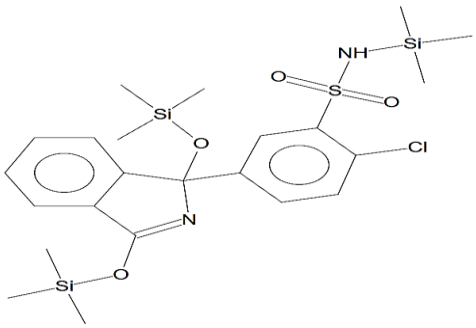	treat high blood pressure and fluid retention caused by various conditions, including heart disease
27.4229	39.6	1,1,3,3,5,5,7,7,9,9,11,11,13,13,15,15-Hexadecamethyloctasiloxane	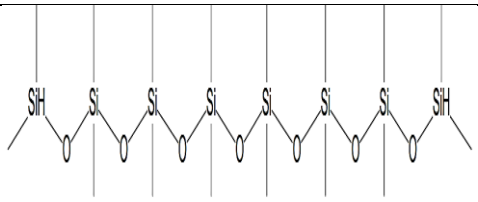	Antimicrobial activity (*Kumaradevan et.al.* 2015, *Boominathan M. and Bakiyalakshmi S.V.* 2016)

28.022	11.9	β-Stigmasterol	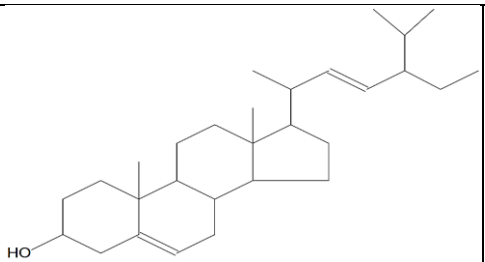	inhibit the development of various cancerous cells by inhibiting the promotion and growth of apoptosis of cancer cells
28.329	13.3	Spherodenon	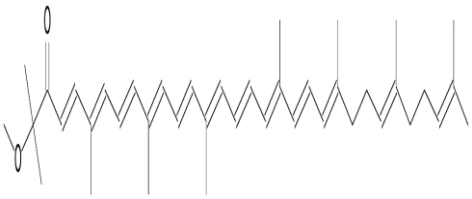	Antioxidant, strongest ability to scavenge free radicals and chemically quench singlet oxygen (*Mein J.R., Lian F. and Wang X.D.* 2019)
28.747	33.0	n-Triacontane		antibacterial, antidiabetic and antitumor activities (*Amudha P. et.al.* 2018)
29.039	57.8	1,1,3,3,5,5,7,7,9,9,11,11,13,13,15,15-Hexadecamethyloctasiloxane	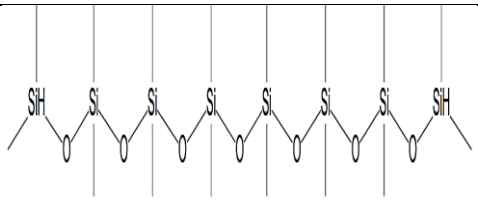	Antimicrobial activity (*Kumaradevan et.al.* 2015, *Boominathan M. and Bakiyalakshmi S.V.* 2016)
30.116	4.55	2,2,4,4,6,6,8,8,10,10,12,12,14,14,16,16-Hexadecamethylcyclooctasiloxane	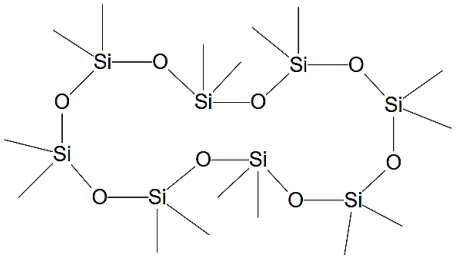	antibacterial activity
30.533	60.3	1,1,3,3,5,5,7,7,9,9,11,11,13,13,15,15-Hexadecamethyloctasiloxane	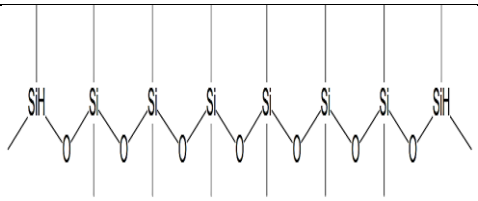	Antimicrobial activity (*Kumaradevan et.al.* 2015, *Boominathan M. and Bakiyalakshmi S.V.* 2016)
31.024	21.5	n-Tetratriacontane		antimicrobial activity (*Afzal M. et.al.* 2014)

31.727	6.66	11,21-Bis[(trimethylsilyl)oxy]pregnane-3,20-dione bis(O-methyloxime)	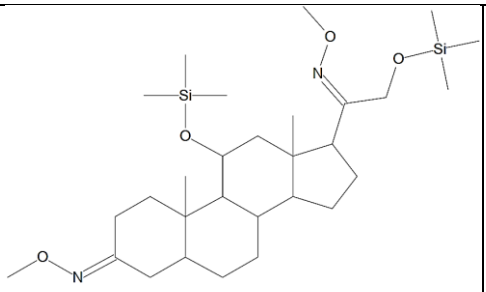	Membrane stabilizer, Energy source and Energy storage
31.961	33.8	1,1,3,3,5,5,7,7,9,9,11,11,13,13,15,15-Hexadecamethyloctasiloxane	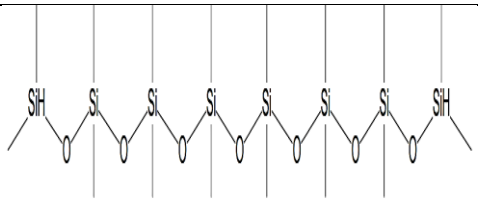	Antimicrobial activity (*Kumaradevan et.al.* 2015, *Boominathan M. and Bakiyalakshmi S.V.* 2016)
32.965	10.1	2,4,6-Trimethyl-2,4,6-triphenyl-1,3,5,2,4,6-trioxatrisilinane	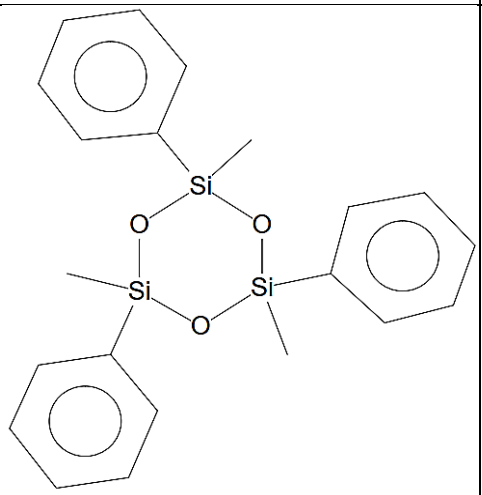	antioxidant property (*Momin K. and Thomas S.C.* 2020)
33.096	6.63	Thymolsulfonephthalein	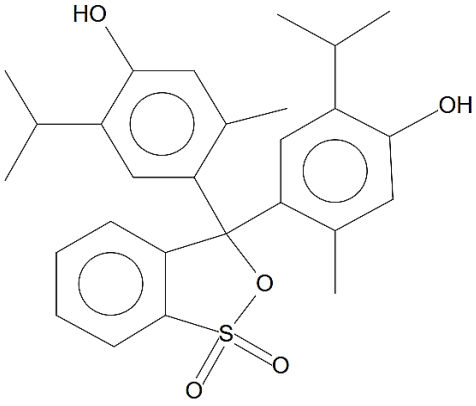	Antibacterial and antifungal activity (*Marchese A. et.al.* 2016)
35.329	21.9	15,17,19,21-Hexatriacontatetrayne	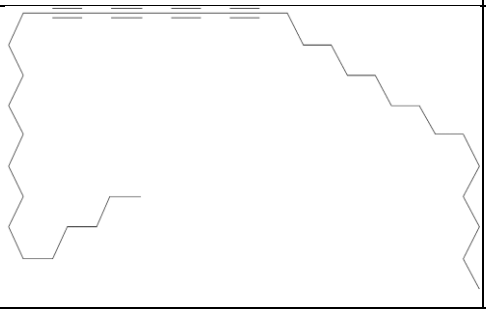	Antiurolithiasis, Antioxidant, Anti-inflammatory, Analgesic, and Diuretic Activity (*Ajay Kumar et.al.* 2021)

35.849	17.6	2-(3-Acetoxy-4,4,10,13,14-pentamethyl-2,3,4,5,6,7,10,11,12,13,14,15,16,17-tetradecahydro-1H-cyclopenta[a] phenanthren-17-yl)-propanoic acid	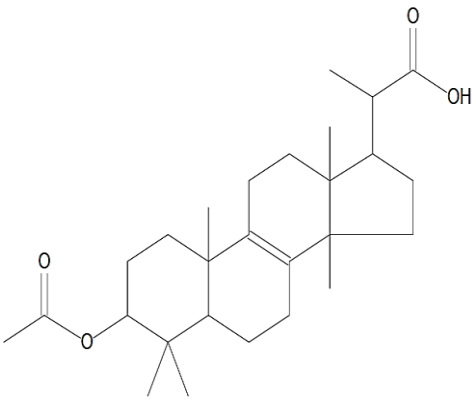	antiinflammatory, anticarcinogenic, antidiabetic, hepatoprotective, antimicrobial, antimycotic, analgesic, immunomodulatory, and cardiotonic activity (*Sandeep and Sumit Ghosh* 2020)
Control biomass				
7.205	19.19	Dodecyl 8-(3-octyl-2-oxiranyl)octanoate	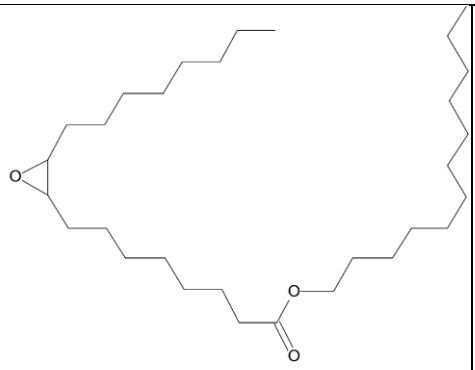	a plant metabolite, a food component, a Daphnia magna metabolite, a human blood serum metabolite and an algal metabolite
15.464	12.65	Cedr-8(15)-ene	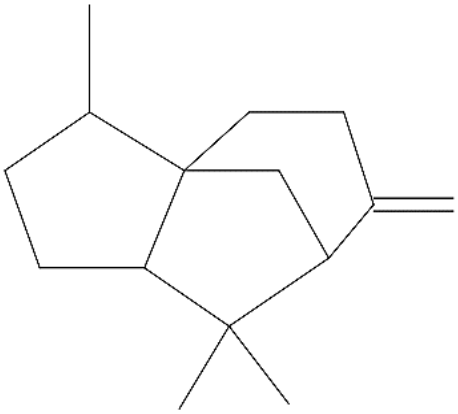	anti-leukemic, antimicrobial and anti-obesity activities

16.394	10.41	1,1,7-Trimethyl-4-methylenedecahydro-1H-cyclopropa[e]azulene-, (1aR,4aR,7R,7aR,7bS)-rel	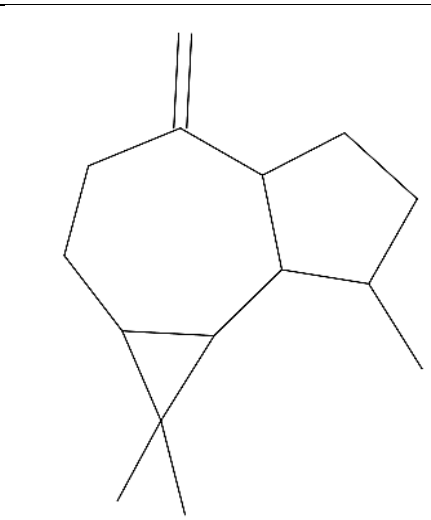	Anticancer, Antioxidant and Antimicrobial activities (*Dahham S.S. et.al.* 2015)
16.687	28.30	Cedr-8(15)-ene	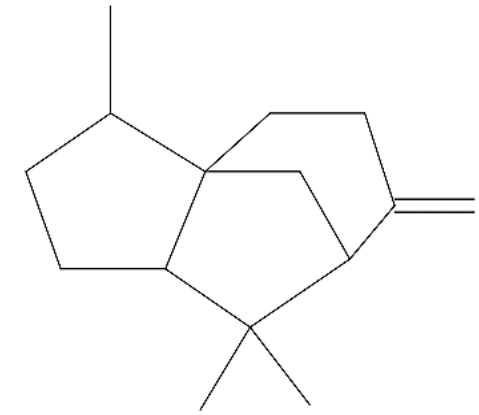	anti-leukemic, antimicrobial and anti-obesity activities
17.038	25.18	α-Muurolene	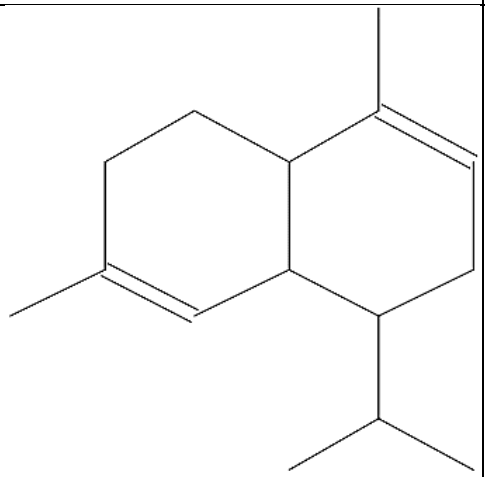	Anti-inflammatory, antioxidant and antimalarial activities (*Afoulous S. et.al.* 2013)

17.309	8.62	β-copaene	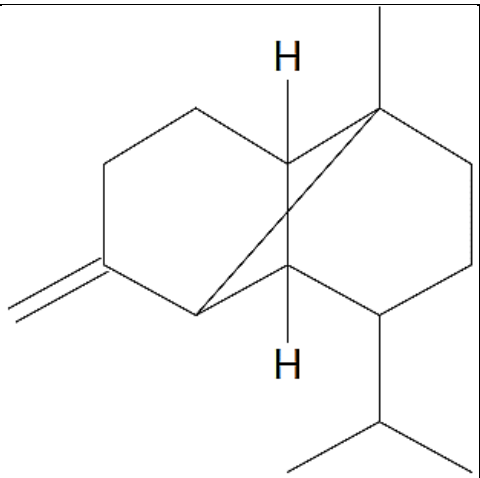	cytotoxic, genotoxic/antigenotoxic and antioxidant/oxidant activity (*Türkez H., Çelik K. and Toğar B.* 2014)
17.478	67.13	Acetamide, 2-[(4-fluorobenzenesulfonyl)(methyl)amino]-N-phenethyl	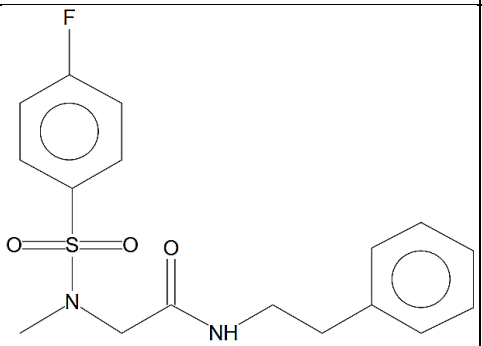	treat glaucoma, oedema (fluid retention), epilepsy, and to treat and prevent altitude/mountain sickness
18.701	87.60	1-Propyltridecyl trifluoroacetate	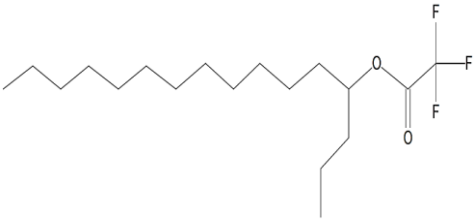	Anti-microbial (*Sarada K. , Jothibai Margret R. and Mohan V.R.* 2011)
19.279	24.79	1-(2-Hydroxy-7,9a,11b-trimethylhexadecahydrocyclopenta[1,2]phenanthro[8a,9-b]oxiren-9-yl)ethanone	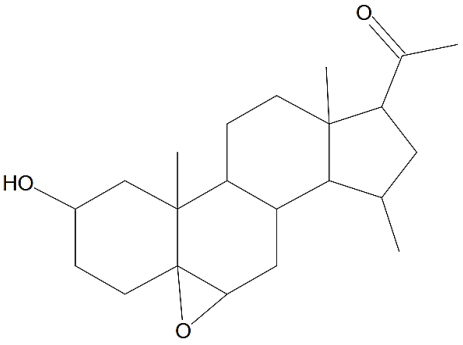	neuroprotective, antimicrobial, and antitumoral activities (*Gerstmeier J. et.al.* 2019)

19.447	25.74	3-(Methoxymethoxy)-3,7,16,20-tetramethyl-1,7,11,15,19-henicosapentaene	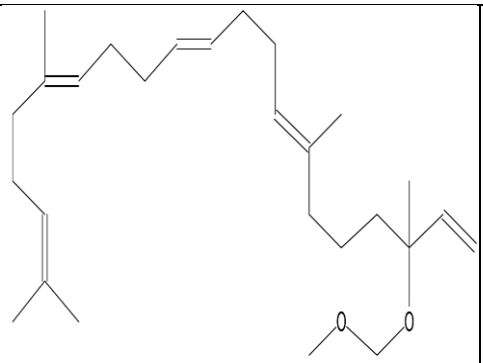	suppressing the production of IgA by B cells, directing the migration of activated B cells in the germinal follicle, and controlling the differentiation of monocytes into macrophages (*McDonald J.G. and Russell D.W.* 2010)
20.158	32.08	6-Hydroxy-4-methyl-1-pentyltetrahydro-2(1H)-pyrimidinethione	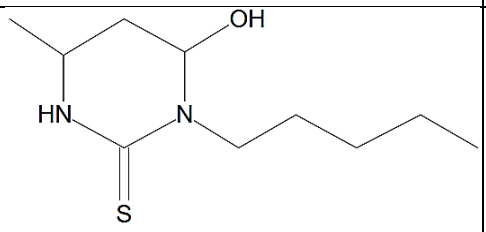	Anthelmintic activity
21.607	100.00	13-Methyl-14-nonacosene	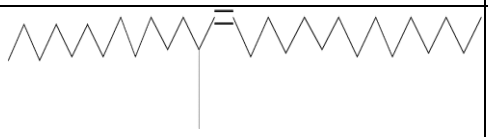	Antibacterial and antioxidant activity (*Abdelshafeek K.A. et.al.* 2010)
23.731	37.16	Methyl 3-hydroxy-2-tetradecyloctadecanoate	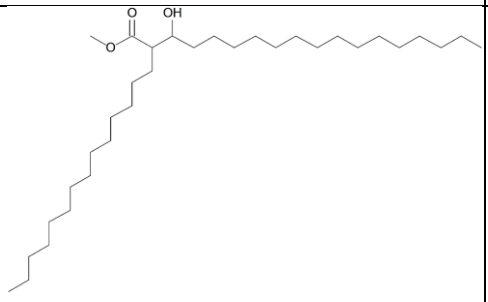	anti-inflammatory activities (*Silva R.O. et.al.* 2014, *Siswadi S. and Saragih G.S.* 2021)
24.251	84.84	2-Hexyldecanol	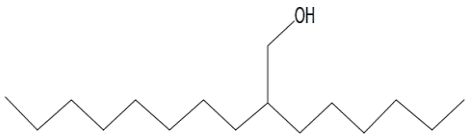	A regulator of ubiquitin–proteasome activity (*Hakozaki T. et.al.* 2013)
25.913	58.56	9-Octadecenoic acid (Z)-, eicosyl ester	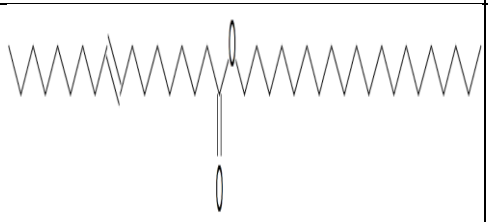	Antiinflammatory, cancer preventive, dermatitigenic, hypocholesterolemic, anemiagenic, insectifuge (*Jainab N.H. and Raja M.K.M.M.* 2017)
26.689	51.41	Dotriacontyl 2,2,2-trifluoroacetate	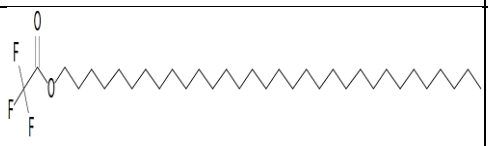	Antioxidant activity (*Erwin E. et.al.* 2019)

28.922	58.73	1,3-Dioctadecyloxypropane	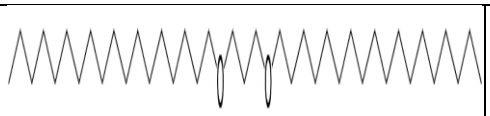	Antioxidant activity

5.17 **ECOTOXICITY:** Following parameters were evaluated to assess the impact of polluted soils on earthworms: mortality, morphology, and death rate. The weight of the earthworms was measured at the start of the experiment, after 7 days, and at the end of the exposure period. Earthworms were cleaned in distilled water and carefully dried on filter paper. The changes in biomass were reported as a percentage of the starting biomass. Fig.5.22 and 5.23 illustrates the length and weight of earthworm respectively and Table 5.11(a–d) illustrates the statistical count of earthworms taken periodically.

5.17.1 ***Survival Studies****:* The number of live earthworms was kept track of, in order to understand if there is mortality in the earthworms due to the subjection to *Lemna minor* biomass. This was done periodically at the start of each week. Significant weight loss was found in *Eudrilus euginiae* treated with a sublethal dosage of *Lemna minor* biomass, and the effects were dose dependent. The weight loss is related to the discharge of bodily fluids under stressful conditions (Espinoza-Navarro et al., 2013) **(Yasha and Vineeta 2021)**.

5.17.2 ***Morphology Studies:*** Morphology studies were carried out at one-week interval. The length and weight of the earthworms were measured four times over the course of the investigation. The earthworms' overall appearance, including signs of discoloration and swelling, and lesions in the body, was observed. In a study on the toxicities of *Lemna minor* biomass on the earthworm *Eudrilus euginiae*, it was found that the worms exhibited coiling and curling, excessive lifting of the body, indicating stress caused by the exposure, the worms moved slowly, and after some time, lesions on the body appeared **(Yasha and Vineeta 2021)**.

Fig: 5.24 Length of Earthworm

Fig: 5.25 Weight of Earthworm

Table 5.11: Control Tray 1

Day 1	**Alive**	10
	Dead	0
Day 2	**Alive**	9
	Dead	1
Day 3	**Alive**	9
	Dead	1
Day 4	**Alive**	8
	Dead	2
Day 5	**Alive**	8
	Dead	2
Day 6	**Alive**	8
	Dead	2
Day 7	**Alive**	9
	Dead	1
Day 8	**Alive**	8
	Dead	2
Day 9	**Alive**	7
	Dead	3
Day 10	**Alive**	7
	Dead	3
Day 11	**Alive**	7
	Dead	3
Day 12	**Alive**	7
	Dead	3
Day 13	**Alive**	8
	Dead	2
Day 14	**Alive**	7
	Dead	3

Average mortality rate = $\frac{Total\ No.of\ dead\ earthworms}{No.of\ total\ earthworms\ in\ 14\ days} \times 100 = \frac{28}{10} \times 100 = 28\%$

Control Tray-1	Day 1		Day 7		Day 14	
Earthworms	**Length**	**Weight**	**Length**	**Weight**	**Length**	**Weight**
1	15	2	7	0.305	7	0.460
2	10	0.303	8	0.308	6	0.445
3	7	0.303	7.5	0.301	6.5	0.193
4	3	1.12	8	0.312	5	0.261
5	9	0.43	8.5	0.314	6	0.169
6	9	0.424	6	0.250	3	0.154
7	5	0.193	7	0.265	2	0.063
8	5	0.146	7.5	0.268	–	–
9	6	0.791	6.5	0.272	–	–
10	2	1.137	–	–	–	–

Table 5.12: Control Tray 2

Day 1	**Alive**	10
	Dead	0
Day 2	**Alive**	9
	Dead	1
Day 3	**Alive**	9
	Dead	1
Day 4	**Alive**	9
	Dead	1
Day 5	**Alive**	9
	Dead	1

Day 6	**Alive**	9
	Dead	1
Day 7	**Alive**	9
	Dead	1
Day 8	**Alive**	5
	Dead	5
Day 9	**Alive**	5
	Dead	5
Day 10	**Alive**	5
	Dead	5
Day 11	**Alive**	5
	Dead	5
Day 12	**Alive**	5
	Dead	5
Day 13	**Alive**	7
	Dead	3
Day 14	**Alive**	5
	Dead	5

Average mortality rate = $\frac{39}{10} \times 100 = 39\%$

Control Tray-2	**Day 1**		**Day 7**		**Day 14**	
Earthworms	**Length**	**Weight**	**Length**	**Weight**	**Length**	**Weight**
1	6	0.652	2	0.565	10	0.889
2	10	0.460	4	0.528	5	0.235
3	10	0.120	2.25	0.584	7	0.626
4	10	0.500	3	0.624	8	0.576
5	12	0.062	3.5	0.632	4	0.232
6	10	0.062	3	0.645	–	–

7	15	0.725	6	0.458	–	–
8	6	0.582	4	0.495	–	–
9	12	0.737	4.5	0.520	–	–
10	–	–	–	–	–	–

Table 5.13: Biomass Tray 1

Day 1	**Alive**	9
	Dead	1
Day 2	**Alive**	9
	Dead	1
Day 3	**Alive**	8
	Dead	2
Day 4	**Alive**	8
	Dead	2
Day 5	**Alive**	8
	Dead	2
Day 6	**Alive**	8
	Dead	2
Day 7	**Alive**	8
	Dead	2
Day 8	**Alive**	8
	Dead	2
Day 9	**Alive**	7
	Dead	3
Day 10	**Alive**	7
	Dead	3
Day 11	**Alive**	7
	Dead	3

Day 12	**Alive**	7
	Dead	3
Day 13	**Alive**	8
	Dead	2
Day 14	**Alive**	7
	Dead	3

Average mortality rate = $\frac{31}{10} \times 100 = 31\%$

Biomass Tray-1	**Day 0**		**Day 7**		**Day 14**	
Earthworms	**Length**	**Weight**	**Length**	**Weight**	**Length**	**Weight**
1	13	0.907	9	0.312	5.5	0.149
2	8	0.712	5	0.077	9	0.197
3	6	0.822	5	0.107	6	0.227
4	7	0.049	5	0.021	6	0.247
5	5.5	0.100	5	0.151	4	0.151
6	1.2	0.222	6	0.129	5	0.137
7	10	1.106	7	0.155	8	0.261
8	3	0.181	4.6	0.093	–	–
9	10	1.532	–	–	–	–
10	–	–	–	–	–	–

Table 5.14: Biomass Tray 2

Day 1	**Alive**	7
	Dead	3
Day 2	**Alive**	10

	Dead	0
Day 3	**Alive**	9
	Dead	1
Day 4	**Alive**	8
	Dead	2
Day 5	**Alive**	8
	Dead	2
Day 6	**Alive**	7
	Dead	3
Day 7	**Alive**	5
	Dead	5
Day 8	**Alive**	8
	Dead	2
Day 9	**Alive**	7
	Dead	3
Day 10	**Alive**	5
	Dead	5
Day 11	**Alive**	5
	Dead	5
Day 12	**Alive**	5
	Dead	5
Day 13	**Alive**	5
	Dead	5
Day 14	**Alive**	3
	Dead	7

Average mortality rate = $\frac{48}{10} \times 100 = 48\%$

Biomass Tray-2	**Day 0**	**Day 7**	**Day 14**

Earthworms	Length	Weight	Length	Weight	Length	Weight
1	9	0.502	5	0.355	4.5	0.133
2	10	0.100	3.5	0.485	5.5	0.099
3	12	0.048	3.25	0.258	6	0.100
4	9	0.184	3	0.359	–	–
5	5	0.554	2.5	0.361	–	–
6	10	0.700	–	–	–	–
7	7	0.382	–	–	–	–
8	–	–	–	–	–	–
9	–	–	–	–	–	–
10	–	–	–	–	–	–

5.18 PREPARATION OF ADSORBENT TABLET PRESS:

Degradation of Methyl Orange by *Lemna minor* is confirmed by preparing the tablet press and compresses powders into tablets of uniform size, shape, and weight containing approximately the same quantity of Active Pharmaceutical Ingredient (API) and excipients.

Fig: 5.26: Adsorbent Tablet Press (ASP Adsorbent)

6 SUMMARY AND CONCLUSION

The duckweed biosorbent was successfully utilized in the removal of Methyl Orange dye, with a maximum removal efficiency of 98.5%. SEM and FTIR spectroscopy were used to examine the morphological properties of rough and porous nature with multiple functional entities such as hydroxyl, amino, carboxyl and alkyl stretches respectively. GCMS revealed the existence of the hydroxyquinone group, which is crucial in the breakdown of dye molecules. *Lemna minor* may be used efficiently as an adsorbent to remove Methyl Orange from aqueous solutions. The choice of activation is determined by contact duration and temperature. The kinetics of pollutant uptake must be studied in order to establish the best operating parameters for full-scale batch procedures. The current study revealed that duckweed is a promising plant for the bioaccumulation of basic dye from aqueous solution at a variety of concentrations. The dye uptake capacity increased with increasing solution concentration and contact duration, and the equilibrium values corresponded extremely well with the Temkin adsorption isotherm. The operating parameters, pH of the solution, biomass dose, temperature and starting dye concentration were shown to have an influence on the biosorption effectiveness of methyl orange dye. Finally, *Lemna minor* being a readily accessible adsorbent can be employed as an alternative to more expensive adsorbents used for dye removal in wastewater treatment procedures. Further studies should be carried out under controlled conditions using *L. minor* ponds for the treatment of artificial textile wastewater using the same dyes after adjusting operating parameters that may impact dye removal efficiency, concentration, contact time and pH value. Simultaneously, plant absorption, microbial degradation, and particle sedimentation processes might be studied in greater depth. More study should be done on the management of different dyes in pond systems planted with *L. minor* or other macrophytes.

REFERENCES:

01. Al Farraj, D.A., Elshikh, M.S., Al Khulaifi, M.M., Hadibarata, T., Yuniarto, A. and Syafiuddin, A. (2019). Biotransformation and detoxification of antraquione dye green 3 using halophilic Hortaea sp. Int Biodeterior Biodegrad 140:72–77. https://doi.org/10.1016/j.ibiod.2019.03.011

02. Amare, E., Kebede, F., Berihu, T. and Mulat, W. (2018) Field-Based Investigation on Phytoremediation Potentials of Lemna minor and Azolla filiculoides in Tropical, Semiarid Regions: Case of Ethiopia. Int. J. Phyto. 20, 965-972. https://doi.org/10.1080/15226514.2017.1365333

03. Archin, S., Sharifi, S.H. and Asadpour, G. (2019). Optimization and modeling of simultaneous ultrasound-assisted adsorption of binary dyes using activated carbon from tobacco residues: response surface methodology. J Clean Prod 239.https://doi.org/10.1016/j.jclepro.2019.118136

04. Aubert, S., Schwitzgue´bel, J.P. (2004). Screening of plant species for the phytotreatment of wastewater containing sulphonated anthraquinones. Water Res. 38, 3569–3575.

05. Balarak, D., Pirdadeh, F., & Mahdavi, Y. (2015). Biosorption of Acid Red 88 dyes using dried Lemna minor biomass.

06. Can-Terzi, B., Goren, A. Y., Okten, H. E., & Sofuoglu, S. C. (2021). Biosorption of methylene blue from water by live Lemna minor. Environmental Technology & Innovation, 22, 101432. doi:10.1016/j.eti.2021.101432

07. Ceschin, S., Crescenzi, M. & Iannelli, M.A. (2020). Phytoremediation potential of the duckweeds Lemna minuta and Lemna minor to remove nutrients from treated waters. Environ Sci Pollut Res 27:15806–15814. https://doi.org/10.1007/s11356-020-08045-3

08. Chadha, A., Florentine, S.K., Chauhan, B.S., Long, B. and Jayasundera, M. (2019) Influence of soil moisture regimes on growth, photosynthetic capacity, leaf biochemistry and reproductive capabilities of the invasive agronomic weed; Lactuca serriola. PLOS ONE 14(6): e0218191. https://doi.org/10.1371/journal.pone.0218191

09. Chakravarty, S., Pimple, S., Chaturvedi, H.T., Singh, S. and Gupta, K.K. (2008). Removal of copper from aqueous solution using newspaper pulp as an adsorbent. J. Hazard. Mater. 159:396-403. https://doi.org/10.1016/j.jhazmat.2008.02.030

10. Chakravarty, S., Pimple, S., Chaturvedi, H.T., Singh, S., Gupta, K.K., 2008. Removal of copper from aqueous solution using newspaper pulp as an adsorbent. J. Hazard. Mater., 159, 396-403.

11. Chandanshive, V., Kadam, S., Rane, N., Jeon, B.-H., Jadhav, J., & Govindwar, S. (2020). In situ textile wastewater treatment in high rate transpiration system furrows planted with aquatic macrophytes and floating phytobeds. Chemosphere, 126513. doi:10.1016/j.chemosphere.2020.12

12. Chatoui, K., Talbaoui, A., Aneb, M., Bakri, Y., Hicham, H. & Tabyaoui, M. (2016). Phytochemical Screening, Antioxidant and Antibacterial activity of Lepidium sativum seeds from Morocco. 7. 2938-2946.

13. Cowan, M. M. (1999) “Plant products as antimicrobial agents,” Clinical Microbiology Reviews, 12(4):564–582.

14. CVB Veevoedertabel 2019 - Chemische samenstellingen en nutritionele waarden van voedermiddelen. https://www.cvbdiervoeding.nl/pagina/10081/downloads.aspx (accessed 2021-05- 21).

15. D. L. Topping and P. M. Clifton, “Short-chain fatty acids and human colonic function: roles of resistant starch and nonstarch polysaccharides,” Physiological Reviews, 81(3):1031–1064, 2001.

16. D. T. Gordon, D. Stoops, and V. Ratliff, Dietary Fiber and Mineral Nutrition, Eagan Press, Eagan, MN, USA, 1995.

17. Dhaif-Allah, M.A.H., Taqui S.N., Syed, U.T. and Syed, A.A. (2020). Kinetic and isotherm modeling for acid blue 113 dye adsorption onto low-cost nutraceutical industrial fenugreek seed spent. Appl Water Sci 10:1–16. https://doi.org/10.1007/s13201-020-1141-3

18. Diyanati, R.A., Balarak, D., 2013. Survey of efficiency agricultural weast in removal of acid orange 7(AO7) dyes from aqueous solution: kinetic and equilibrium study: Iran. J. Health. Sci., 2(1), 35-40.

19. Dogan, M., Abak, H. and Alkan, M. (2008). Biosorption of methylene blue from Aqueous solutions by hazelnut shells: Equilibrium, Parameters and Isotherms. Water. Air. Soil. Poll. 192(1):141-53. http://dx.doi.org/10.1007/s11270-008-9641-z

20. Edziri, H., Mastouri, I., Chéraif, M. and Aouni, M. (2010) “Chemical composition and antibacterial, antifungal and antioxidant activities of the flower oil of Retama raetam (Forssk) Webb from Tunisia,” Natural Product Research, 24(9):789–796.

21. Ekperusi, A. O., Sikoki, F. D. and Nwachukwu, E. O. (2019). Application of common duckweed (Lemna minor) in phytoremediation of chemicals in the environment: State and future perspective. Chemosphere, 223:285–309. doi:10.1016/j.chemosphere.2019.02

22. Ekperusi, A. O., Sikoki, F. D., & Nwachukwu, E. O. (2019). Application of common duckweed (Lemna minor) in phytoremediation of chemicals in the environment: State and future perspective. Chemosphere, 223, 285–309. doi:10.1016/j.chemosphere.2019.02

23. Ge, X., Zhang, N., Phillips, G.C. and Xu, J. (2012). Growing Lemna minor in agricultural wastewater and converting the duckweed biomass to ethanol. Bioresour Technol. 124:485-488. doi: 10.1016/j.biortech.2012.08.050

24. Ge, X., Zhao, X. and Bai, F. (2005). Online monitoring and characterization of flocculating yeast cell flocs during continuous ethanol fermentation. Biotechnol. Bioeng. 90, 523–531. https://doi.org/10.1002/bit.20391

25. Ghazali, A., Yusuf, B., Montakhab, A. & Thamer, M. (2013). Estimation of vegetation porosity in vegetated waterways. Proceedings of the ICE - Water Management. 166. 333-340. 10.1680/wama.11.00058.

26. Hanif MA, Nadeem R, Bhatti HN, Rashid N, Ahmad NR, Ansari TM, Ni(II) biosorption by Cassia fistula (Golden Shower) biomass, J. Hazard. Mater., 2007, 139:345-355.

27. Hassan A. and Ullah, H. (2019) “Antibacterial and antifungal activities of the medicinal plant veronica biloba,” Journal of Chemistry, vol. 2019.

28. Hassan, A., Akmal, Z. and Khan, N. (2020). "The Phytochemical Screening and Antioxidants Potential of Schoenoplectus triqueter L. Palla", Journal of Chemistry.8.

https://doi.org/10.1155/2020/3865139

29. Hattabi, L., Talbaoui, A., Amzazi, S., Bakri, Y., Hicham, H., Costa, J., Desjobert, J. & Tabyaoui, M. (2016). Chemical composition and antibacterial activity of three essential oils from south of Morocco. (Thymus satureoides, Thymus vulgaris and Chamaelum nobilis). 7. 3110-3117.

30. Imron, M. F., Ananta, A. R., Ramadhani, I. S., Kurniawan, S. B., & Abdullah, S. R. S. (2021). Potential of Lemna minor for removal of methylene blue in aqueous solution: Kinetics, adsorption mechanism, and degradation pathway. Environmental Technology & Innovation, 24, 101921. doi:10.1016/j.eti.2021.101921

31. Imron, M.F., Ananta, A.R., Ramadhani, I.S., Kurniawan, S.B. and Abdullah, S.R.S. (2021). Potential of Lemna minor for removal of methylene blue in aqueous solution: Kinetics, adsorption mechanism, and degradation pathway. Env. Tech. & Inn. 24:01921. doi:10.1016/j.eti.2021.101921

32. Jin, X., Shi, C., Yu, C.Y., Yamada, T. and Sacks, E.J. (2017). Determination of Leaf Water Content by Visible and Near-Infrared Spectrometry and Multivariate Calibration in Miscanthus. Front. Plant Sci. 8:721. https://doi.org/10.3389/fpls.2017.00721

33. Kaur, L., Gadgil, K. and Sharma, S. (2012). Role of pH in the Accumulation of Lead and Nickel by Common Duckweed (Lemna minor). Int. J. Bioassays. 1(12):191-195

34. Khandare, R. V., & Govindwar, S. P. (2015). Phytoremediation of textile dyes and effluents: Current scenario and future prospects. Biotechnology Advances, 33(8), 1697–1714. doi:10.1016/j.biotechadv.2015.09.

35. Lodeiro P, Barriada JL, Herrero R, Sastre de Vicente ME, The marine macroalga Cystoseira baccata as biosorbent for cadmium(II) and lead(II) removal: kinetic and equilibrium studies, Environ Pollut, 2006, 142:264-273.

36. Mamtha, B., Kavitha, K., Srinivasan, K. K. and Shivananda, P. G. (2004) “An in vitro study of the effect of Centella asiatica [Indian pennywort] on enteric pathogens,” Indian Journal of Pharmacology, 36(1):41.

37. Maqbool, M., Bhatti, H.N., Sadaf, S., Al-Anazy, M.M. and Iqbal, M. (2020). Biocomposite of

polyaniline and sodium alginate with Oscillatoria biomass: a potential adsorbent for the removal of basic blue 41. J. Mater. Res. Technol. 9(6): 14729-14741. https://doi.org/10.1016/j.jmrt.2020.10.017

38. Marimuthu, S., Antonisamy, A. J., Malayandi, S., Rajendran, K., Tsai, P.-C., Pugazhendhi, A., & Ponnusamy, V. K. (2020). Silver nanoparticles in dye effluent treatment: A review on synthesis, treatment methods, mechanisms, photocatalytic degradation, toxic effects and mitigation of toxicity. Journal of Photochemistry and Photobiology B: Biology, 205, 111823. doi:10.1016/j.jphotobiol.2020.111

39. Marimuthu, S., Antonisamy, A.J., Malayandi, S., Rajendran, K., Tsai, P.-C., Pugazhendhi, A. and Ponnusamy, V.K. (2020). Silver nanoparticles in dye effluent treatment: A review on synthesis, treatment methods, mechanisms, photocatalytic degradation, toxic effects and mitigation of toxicity. J. Photochem. Photobiol. B: Biol. 205:111823. doi:10.1016/j.jphotobiol.2020.111

40. McLay, C.L. (1976). The effect of pH on the population growth of three species of duckweed: Spirodela oligorrhiza, Lemna minor and Wolffia arrhiza. Freshwat. Biol. 6:125–136. https://doi.org/10.1111/j.1365-2427.1976.tb01596.x

41. Mengistu, A., Mavimbela, S. & Rensburg, L. (2018). Characterisation of the soil pore system in relation to its hydraulic functions in two South African aeolian soil groups. South African Journal of Plant and Soil. 36. 1-10. 10.1080/02571862.2018.1487594.

42. Neag, E., Malschi, D. and Măicăneanu, A. (2018). Isotherm and kinetic modelling of Toluidine Blue (TB) removal from aqueous solution using Lemna minor. Int. J. Phytoremediation 20(10):1049–1054. https://doi.org/10.1080/15226514.2018.1460304

43. Nieuwland, M., Geerdink, P., Engelen-Smit, N.P.E., van der Meer, I.M., America, A.H.P., Mes, J.J., Kootstra, A.M.J., Henket, J.T.M.M., and Mulder, W.J. (2021). Isolation and Gelling Properties of Duckweed Protein Concentrate. ACS Food Science & Technology. 1(5):908-916. DOI: 10.1021/acsfoodscitech.1c00009

44. Othaman, N., Isa, M.D., Nazrin, M., Murad, Z., Anuar, S., Harun, A., Mohyar, S.N. (2020). Electrical conductivity (EC) sensing system for paddy plant using the internet of things (IoT) connectivity. AIP Conference Proceedings. 2203. 020005. 10.1063/1.5142097.

45. P'ei, C. and Chen, S. (1982) "Verbenaceae," Flora Reipublicae Popularis Sinicae, 65(1):1–49.

46. Prakash, P., Kumar, J. A., Dhandapani, B., Hrishitha Sree, S., Madhumeena, S., Lavanya, Y. and Inbathamizh, L. (2021). Utilization of eutrophicated Lemna minor for biosorption of acid blue dye. Biomass Conv. Bioref. https://doi.org/10.1007/s13399-021-02024-5

47. R. Alghazeer, H. El-Saltani, N. Saleh, A. Al-Najjar, and F. Hebail, "Antioxidant and antimicrobial properties of five medicinal Libyan plants extracts," Natural Science, 4(5):324–335, 2012.

48. Reema, R.M., Saravanan, P., Kumar, M.D. and Renganathan, S. (2011). Accumulation of methylene blue dye by growing Lemna minor. Sep Sci Technol 46:1052–1058. https://doi.org/10.1080/01496395.2010.528503

49. Reyes-Ledezma, J. L., Uribe-Ramírez, D., Cristiani-Urbina, E., & Morales-Barrera, L. (2020). Biosorptive removal of acid orange 74 dye by HCl-pretreated Lemna sp. PLOS ONE, 15(2), e0228595. doi:10.1371/journal.pone.0228595

50. Reyes-Ledezma, J.L., Uribe-Ramírez, D., Cristiani-Urbina, E. and Morales-Barrera, L. (2020). Biosorptive removal of acid orange 74 dye by HCl-pretreated Lemna sp. PLOS ONE, 15(2):0228595. doi:10.1371/journal.pone.0228595

51. Sag Y, Kaya A, Kutsal T, The simultaneous biosorption of Cu and Zn on Rhizopus arrhizus: application of the adsorption models, Hydrometallurgy, 1998, 50:297-314.

52. Samrot, A.V., Mathew, A.A., Shylee, L., Hemalatha, N. and Karunya, A. (2009). Evaluation Of Bioactivity of Various Indian Medicinal Plants – An In-Vitro Study. Int J Int Med. 8(2)

53. Sanjoaquin, M. A., Appleby, P. N., Spencer, E. A. and Key, T. J. (2004) "Nutrition and lifestyle in relation to bowel movement frequency: a cross-sectional study of 20 630 men and women in EPIC-Oxford," Public Health Nutrition, 7(1):77–83.

54. Sato Y, Shibata H, Arai T, Yamamoto A, Okimura Y, Arakaki N and Higuti T. (2004). Variation in synergistic activity by flavone and its related compounds on the increased susceptibility of various strains of methicillin-resistant Staphylococcus aureus to beta-lactam antibiotics. Int J Antimicrob Agents. 24(3):226-233. doi: 10.1016/j.ijantimicag.2004.02.028.

55. Savithramma, N., Rao, M. L. and Suhrulatha, D. (2011) "Screening of medicinal plants for

secondary metabolites," Middle-East Journal of Scientific Research, 8(3):579–584.

56. Sharifi-Rad, J. (2016) "Herbal antibiotics: moving back into the mainstream as an alternative for superbugs," Cellular and Molecular Biology, 62(9):1-2.

57. Smitha, T., Santhi, T., Prasad, A.L. and Manonmani, S. (2017). Cucumis sativus used as adsorbent for the removal of dyes from aqueous solution. Arab J Chem 10:S244–S251. https://doi.org/10.1016/j.arabjc.2012.07.030

58. Sudarjanto, G., Keller-Lehmann, B. and Keller, J. (2006). Optimization of integrated chemical-biological degradation of a reactive azo dye using response surface methodology. J Hazard Mater 138:160–168. https://doi.org/10.1016/j.jhazmat.2006.05.054

59. T. Lu, "Potential health benefits and problems associated with antinutrients in foods," Food Research International, 26(2):131–148, 1993.

60. T. P. T. Cushnie and A. J. Lamb, "Antimicrobial activity of flavonoids," International Journal of Antimicrobial Agents, vol. 26, no. 5, pp. 343–356, 2005.

61. Uddin, M.K. and Baig, U. (2019). Synthesis of Co3O4 nanoparticles and their performance towards methyl orange dye removal: characterisation, adsorption and response surface methodology. J Clean Prod 211:1141–1153. https://doi.org/10.1016/j.jclepro.2018.11.232

62. Uysal, Y. (2013). Removal of chromium ions from wastewater by duckweed, Lemna minor L. by using a pilot system with continuous flow. J Hazard Mater. 263(2):486-492. https://doi.org/10.1016/j.jhazmat.2013.10.006

63. Vishnu, D. and Dhandapani, B. (2020). Integration of Cynodon dactylon and Muraya koenigii plant extracts in amino-functionalised silica-coated magnetic nanoparticle as an effective sorbent for the removal of chromium(VI) metal pollutants. IET Nanobiotechnol 14:449–456. https://doi.org/10.1049/iet-nbt.2019.0313

64. Yadav, Y. and Shukla, V. (2021). Role of Earthworms in Soil Ecotoxicology Assessment Studies.

65. Yang, S.J. and De Jong, E., 1971. Effect of soil water potential and bulk density on water uptake patterns and resistance to flow of water in wheat plants. Can. J. Soil Sci., 51: 211--220.

66. Yaseen, D. A., & Scholz, M. (2016). Shallow pond systems planted with Lemna minor treating azo dyes. Ecological Engineering, 94, 295–305. doi:10.1016/j.ecoleng.2016.05.081

67. Yaseen, D.A. and Scholz, M. (2016). Shallow pond systems planted with Lemna minor treating azo dyes. Ecol. Engg. 94:295–305. doi:10.1016/j.ecoleng.2016.05.081

68. Yu, G., Liu, H., Venkateshan, K., Yan, S., Cheng, J., Sun, X.S. & Wang, D. (2011). Functional, physiochemical, and rheological properties of duckweed (Spirodela polyrhiza) protein. Transactions of the ASABE. 54. 555-561. 10.13031/2013.36459.

Curiginal

Document Information

Analyzed document	Swathy T - Thesis .docx (D133972340)
Submitted	2022-04-19T16:33:00.0000000
Submitted by	Dr.Prakash Pandurangan
Submitter email	prakash.biotech@sathyabama.ac.in
Similarity	4%
Analysis address	prakash.biotech.sathya@analysis.urkund.com

Sources included in the report

SA **Ms_BJPR_28521 1-8-16.pdf**
Document Ms_BJPR_28521 1-8-16.pdf (D21269912) 1

W URL: https://escholarship.org/content/qt18x2377v/qt18x2377v_noSplash_35fbbdfc5cc63a0b7fef26bd39f7c12c.pdf?t=r1y6bb
Fetched: 2022-04-19T16:34:32.1270000 2

SA **Manuscript version 2 (1).docx**
Document Manuscript version 2 (1).docx (D111330943) 2

SA **New file.docx**
Document New file.docx (D111329741) 1

Curiginal

Hit and source - focused comparison, Side by Side

Submitted text As student entered the text in the submitted document.

Matching text As the text appears in the source.

1/6	SUBMITTED TEXT	28 WORDS	100%	MATCHING TEXT	28 WORDS
Temkin isotherm equilibrium binding constant (l/g) b – Temkin isotherm constant			Temkin isotherm equilibrium binding constant (L/g) B= Temkin isotherm constant		

SA Ms_BJPR_28521 1-8-16.pdf (D21269912)

2/6	SUBMITTED TEXT	1933 WORDS	100%	MATCHING TEXT	1933 WORDS
ppm 0.199 3.25 12 36000 0.25 1 0.000862 200 ppm 0.203 3.25 12 36000 0.25 1 0.00088 300 ppm 0.169 3.25 12 36000 0.25 1 0.000732 400 ppm 0.246 3.25 12 36000 0.25 1 0.001066 500 ppm 0.204 3.25 12 36000 0.25 1 0.000884 600 ppm 0.229 3.25 12 36000 0.25 1 0.000992 700 ppm 0.264 3.25 12 36000 0.25 1 0.001144 800 ppm 0.201 3.25 12 36000 0.25 1 0.000871 900 ppm 0.021 3.25 12 36000 0.25 1 0.000091 1000 ppm 0.299 3.25 12 36000 0.25 1 0.001296 1100 ppm 0.25 3.25 12 36000 0.25 1 0.001083 1200 ppm 0.165 3.25 12 36000 0.25 1 0.000715 1300			ppm ppm ppm ppm ppm ppm ppm ppm ppm ppm ppm ppm		

W https://escholarship.org/content/qt18x2377v/qt18x2377v_noSplash_35fbbdfc5cc63a0b7fef26bd39f7c12c. ...

3/6	SUBMITTED TEXT	1933 WORDS	100%	MATCHING TEXT	1933 WORDS
ppm 0.438 3.25 12 36000 0.25 1 0.001898 200 ppm 0.254 3.25 12 36000 0.25 1 0.001101 300 ppm 0.273 3.25 12 36000 0.25 1 0.001183 400 ppm 0.452 3.25 12 36000 0.25 1 0.001959 500 ppm 0.196 3.25 12 36000 0.25 1 0.000849 600 ppm 0.209 3.25 12 36000 0.25 1 0.000906 700 ppm 0.365 3.25 12 36000 0.25 1 0.001582 800 ppm 0.448 3.25 12 36000 0.25 1 0.001941 900 ppm 0.329 3.25 12 36000 0.25 1 0.001426 1000 ppm 0.386 3.25 12 36000 0.25 1 0.001673 1100 ppm 0.294 3.25 12 36000 0.25 1 0.001274 1200 ppm 0.255 3.25 12 36000 0.25 1 0.001105 1300			ppm ppm ppm ppm ppm ppm ppm ppm ppm ppm ppm ppm		

W https://escholarship.org/content/qt18x2377v/qt18x2377v_noSplash_35fbbdfc5cc63a0b7fef26bd39f7c12c. ...

Curiginal

4/6	SUBMITTED TEXT	24 WORDS	100%	MATCHING TEXT	24 WORDS

Khandare, R. V., & Govindwar, S. P. (2015). Phytoremediation of textile dyes and effluents: Current scenario and future prospects. Biotechnology Advances, 33(8), 1697–1714.

SA Manuscript version 2 (1).docx (D111330943)

5/6	SUBMITTED TEXT	15 WORDS	100%	MATCHING TEXT	15 WORDS

Govindwar, S.P. (2015). Phytoremediation of textile dyes and effluents: Current scenario and future prospects.

SA Manuscript version 2 (1).docx (D111330943)

6/6	SUBMITTED TEXT	31 WORDS	64%	MATCHING TEXT	31 WORDS

adsorbent for the removal of dyes from aqueous solution. Arab J Chem 10:S244–S251. https://doi.org/10.1016/j.arabjc.2012.07.030 28. Reema, R.

SA New file.docx (D111329741)